Zermelo Navigation Problems on Surfaces of Revolution and Hamiltonian Dynamics

Bernard Bonnard, Olivier Cots, Boris Wembe

Zermelo Navigation Problems on Surfaces of Revolution and Hamiltonian Dynamics

B. Bonnard[*], O. Cots[†], B Wembe[‡]

May 7, 2021

Abstract

In this article, using the historical example from Carathéodory-Zermelo and a recent work describing the evolution of a passive tracer in a vortex, we present the geometric frame to analyze Zermelo navigation problems on surfaces of revolution, assuming the current invariant by symmetry of revolution. In this context, normal (polar) coordinates distinguish parallels and meridians and one will consider the case where the current is oriented along the parallels. The problem is set in the frame of time optimal control and the Maximum Principle allows to select minimizers among geodesics, solutions of an Hamiltonian dynamics. In the strong current domain, there exist both normal and abnormal geodesics, the later representing limit curves of the cone of admissible directions. We present the concepts of conjugate points in the normal and abnormal directions, associated to the singularity analysis of the central field defined by the Lagrangian manifold formed by geodesics curves with fixed initial conditions, in relation with Hamilton-Jacobi equation. This leads to a parameterization of the conjugate locus in the general case and conjugate points along abnormal directions are cusp points of the geodesics when crossing the limit of the weak current domain and are associated to non-continuity of the value function, due to bad accessibility propertie in the weak current domain. The dynamics is Liouville integrable but this dynamics is intricated due to non-compactness of the Liouville tori related to separatrices curves and interaction between parallels geodesics causing the existence of Reeb components. We present a generalized Morse-Reeb classification associated to an extended potential and this leads to a stratification of the geodesics set. Another complementary point of view is described which goes back to the historical example, using the parameterization of the geodesics by the heading angle of the ship, corresponding to the so-called Goh transformation in optimal control. This leads to a different stratification of the set of geodesics using Lie brackets computations and integration with Clairaut relation, interpreted as computing the control given by the derivative of the heading angle. The abnormal geodesics being seen as a projection with two branches of a determinantal variety. The final problem is to compute the cut locus and we introduce the first return mappings to equator and meridian to order the geodesics and to compute the separating locus formed by intersecting time minimizing geodesics. We apply our approach to analyse the historical example and a set of cases studies related in particular to Zermelo navigation on spheres of revolution and the generalized vortex case where the different techniques are used to analyze the dynamics of the geodesics and in fine to compute the optimal syntheses in the geodesically complete case.

Key words

Zermelo navigation problems on surface of revolution, Abnormal geodesics, Integrable Hamiltonian dynamics and Morse-Reeb classification, Conjugate and cut loci, Hamilton-Jacobi equation and regularity of the value function.

1 Introduction and Summary

Our aim is to introduce the geometric frame from optimal control viewpoint to analyze *Zermelo naviagation problems on surfaces of revolution* with application to numerous cases studies, motivated by applications. The

---

[*]McTAO, INRIA Sophia Antipolis, Nice, France, `bbonnard@u-bourgogne.fr`
[†]ENSEEIHT, IRIT, Toulouse, France, `olivier.cots@irit.fr`
[‡]Université Paul Sabatier, IRIT, Toulouse, France, `boris.wembe@irit.fr`

first one being the *historical example* due to Carathéodory-Zermelo [22, 42] which is one founding study of classical calculus of variations and which serves as a seminal motivation in our analysis. The second case concerns the displacement of a *passive tracer* in the *neighborhood of a vortex*. This case with singularity has been recently studied in [14, 15], motivated by applications in hydrodynamics [3] and in space and celestial mechanics, in the relation with N-body problem, in the frame of Hamiltonian dynamics [29]. From geometric point of view, the study of Riemannian metrics on surfaces of revolution is an important problem in Riemannian geometry and the determination of the conjugate and cut loci for *convex spheres* goes back to the earliest works by Poincaré and Myers [30, 31, 35]. Only very recently the *conjugate and cut loci* for oblate and prolate *ellipsoids of revolution* were computed, solving the Jacobi conjecture about the astroidal shape of the conjugate locus and later extended to general ellipsoids [27]. This leads to define a series of Zermelo navigation problems on two-spheres of revolution, in the *weak current* case (where the drift current can be compensated) associated to *Randers geometry* [25, 26] where the conjugate and cut loci can be computed by small deformation. But our aim is to extend the analysis beyond the context of *Riemann-Finsler geometry* [5] by considering the *strong current case* (in which the current is with larger norm than the unit Riemannian norm) and in the frame of Hamiltonian dynamics coming form *Maximum Principle* [37]. In this article we shall consider the general case where the ambient manifold M is a surface of revolution endowed with an induced Riemannian metric which can be written $g = dr^2 + m^2(r)d\theta^2$ in (polar)*normal coordinates* with $m(r) > 0$ and the current is defined by a vector field $F_0 = \mu(r)\frac{\partial}{\partial\theta}$, and is oriented only along the parallels (the geometry being defined by the two functions $m(r)$ and $\mu(r)$). Taking the orthonormal frame $F_1 = \frac{\partial}{\partial r}$, $F_2 = \frac{1}{m(r)}\frac{\partial}{\partial\theta}$, from optimal control point of view the Zermelo navigation problems amount to *minimize the transfer time* between two points of the ambient space for the control system

$$\frac{dq}{dt}(t) = F_0(q(t)) + \sum_{i=1,2} u_i()F_i(q(t)), u = (u_1, u_2), \|u\| \le 1. \tag{1}$$

One first contribution of this article being, following Carathéodory-Zermelo point of view, to parameterize the control by the *heading angle* of the ship α , observing that the control can be restricted to $\|u\| = 1$ and setting $u_1 = cos\alpha, u_2 = sin\alpha$. This correspond to *Goh transformation* in optimal control taking as control v the derivative of the heading angle. Using this transformation and Maximum Principle the geodesics candidate as minimizers can be interpreted as *singular trajectories* [11] of a single-input affine control systems. Moreover they can be stratified into *normal geodesics* for which using [17] one can distinguish between small time minimizing or maximizing trajectories, while they are separated by *abnormal geodesics*, called limit curves by Carathéodory-Zermelo. The geodesics flow is *Liouville integrable* and in this frame we provide a neat interpretation of the standard *Clairaut relation* and the integration of the geodesics by quadrature. The stratification of the set of geodesics in this context being related to Lie brackets computations only.

The second contribution of this article is to use again the Maximum Principle to stratify the set of geodesics using a *generalized Morse-Reeb classification* [7], introducing a one-dimensional mechanical systems with and extended potential. This leads to a different stratification of the sets of geodesics in which either they fill *compact tori* described by Liouville-Arnold theorem but also *non-compact* tori. Hence this leads to a complicated Hamiltonian dynamics and in particular this gives a neat interpretation to Reeb components occurence detected in the vortex case [15] and the relation to interactions between *equators* solutions (corrresponding to parallel geodesics).

The third contribution is to apply our different techniques to three cases studies . The first one being the historical example in which the complete analysis relies to the stratification using the heading angle and we recover the time minimal synthesis described in [22]. The second study concerns the deformation of a Riemannian case on a two-sphere of revolution in which we use the stratification of the set of geodesics with the generalized Morse-Reeb classification. The final case being the extension of the vortex case to get complicated Hamiltonian dynamics with several equators solutions and *Reeb components*.

The final contribution being to get a self-contained and neat presentation of the conjugate and cut points for both normal and abnormal directions extending [17] to the abnormal case where the geodesics can have *cusp points* corresponding to conjugate points [10] This is interpreted in terms of *Lagrangian manifolds* [9] and Hamilton-Jacobi equation [28], showing in particular the relation with integrability properties of the geodesics equations and of the value function. The important point remaining efficient algorithms to *effective computations* of the conjugate loci in the case studies, combining in a modern setting mathematical analysis and numerical computations based on [17], HamPathcode (www.hampath.org).

The article is organized as follows. In section 2, we introduce the general concepts and definitions and a large collection of cases studies which are in fine the motivations of our work. In section 3 we introduce the theoretical tools of our article. We recall the Maximum Principle and this leads to two parameterizations of the geodesic curves, the first one is related to the extended Carathéodory-Zermelo-Goh transformation and we construct *semi-normal forms* to parameterize the conjugate and cut loci in the normal and abnormal case. The generalized Gauss curvature is introduced using Jacobi equation, which is useful to estimate conjugate points for equator solutions. The second parameterization is described and leads to define the generalized potential. We introduce the concepts and results related to the generalized Morse-Reeb classification of the geodesics. In the final section 4, we present the applications of our techniques to analyze three cases studies. The first case concerns the historical example for which we present a complete analysis in the frame of geometric control, describing in particular the cut loci related to existence of abnormal curves and associated to non-continuity of the value function and bad accessibility properties. The second case is a Zermelo navigation problem on a two-sphere of revolution associated to *Kepler orbital transfer* but also to the so-called *Grushin case*, where the metric is singular. We use the generalized Morse-Reeb classification and we decribe the conjugate and cut loci for an initial point located on the equator solution. We show in particular the stratification of the cut loci into *two distinct* components associated respectively the branch related to the abnormal solution (already detected in the historical example in relation with limit curves) and the branch occuring in the Riemannian case of revolution and associated to the general description of the conjugate and cut loci by Poincaré. The third case aims to describe complicated dynamics related to generalizations of the single vortex case. Finally a construction is presented to glue all the existing cases either along equators or meridians to get a general classification of situations occuring on surfaces of revolution with a parallel current, opening the road extension to a general current with rotational symmetry.

2   Definitions and Notations. List of the Cases Studies

2.1   Definitions and Notations

Let M be a (smooth) *surface of revolution* and we denote by g the *induced Riemannian metric* $\|\cdot\|_g$ *and let* T^*M be the *cotangent bundle* endowed with *Liouville canonical form* $\alpha = pdq$. A *Lagrangian manifold* is a 2-dimensional submanifold where $d\alpha$ is zero. We denote by (r, θ) *normal (polar) coordinates* on the *covering* Riemannian manifold M^c where the metric takes the form $g = \mathrm{d}r^2 + m^2(r)\,\mathrm{d}\theta^2$, $m(r) > 0$. This defines a canonical *orthonormal frame* $F_1 := \frac{\partial}{\partial r}$, $F_2 := \frac{1}{m(r)}\frac{\partial}{\partial \theta}$. The lines $r=$ constant are called the *parallels* and the lines $\theta =$ constant are called the *meridians*. A *Zermelo navigation problem* is defined by the pair (M, F_0) and where F_0 is a vector field invariant by $\theta-$ rotation, representing the current and oriented along the parallel, so that in the covering space it can be written as $F_0 := \mu(r)\frac{\partial}{\partial \theta}$. If $\mu(r) = v$ constant (resp. linear) this is called the *constant* (resp. *linear*) *current case*. Let $q_0 = (r_0, \theta_0)$, an *adapted neighborhood* of q_0 is a rectangle $R := \{r_1 \leq r \leq r_2; \theta_1 \leq \theta \leq \theta_2\}$. From *control point of view*, a Zermelo navigation problem can be written in $q-$coordinates as : Minimize the transfer time between two points (q_0, q_1) for the system :

$$\frac{dq(t)}{\mathrm{d}t} = F_0(q(t)) + \sum_{i=1,2} u_i(t)F_i(q(t)),$$

where the control $u(\cdot) = (u_1(\cdot), u_2(\cdot))$ is measurable function defined on $[0, T]$, whose (euclidian) norm is $\|u\| = \sqrt{u_1^2 + u_2^2}$ and one may assume $\|u\| \leq 1$. The *heading angle* α of the ship in the canonical frame is defined by: $u_1 = sin\alpha$, $u_2 = \cos\alpha$ where according to Clairaut interpretation, α is the angle with respect to the parallel. One can decompose the covering space with coordinates (r, θ) into rectangles $r_0 < r < r_1$ in which we have either *weak current* if $\|F_0\|_g < 1$ or *strong current* case if $\|F_0\|_g > 1$. Transition between the two cases being called the *moderate currrent* case given $\|F_0\|_g = 1$. The Zermelo navigation problem is called (*geodesically*) complete if for each pair (q_0, q_1) such that q_1 is *accessible* to q_0, there exists a minimizing trajectory of the control system joining q_0 to q$_1$. Fixing the initial point q_0, we denote by $q_1 \to T(q_0, q_1)$ the *time minimal value function* representing the minimized transfer time from q_0 to q_1.

2.2 List of motivating cases studies

2.2.1 Historical example of Carathéodory-Zermelo ([22, 42])

One founding problem in classical *calculus of the variations* is the problem introduced by Carathéodory and Zermelo of a ship navigating on a river aiming to reach the opposite shore in minimum time. Hence M is the 2-dimensional Euclidian space with metric $g = \mathrm{d}x^2 + \mathrm{d}y^2$ in the coordinates $q = (x, y)$, y being the distance to the shore. To make a complete analysis, Carathéodory-Zermelo considered a *linear* current of the form $F_0 = y\frac{\partial}{\partial x}$. Using our notation to fix parallels and meridians, one must set $x = \theta$, $y = r$, so that the ambient manifold is the Euclidian space with metric $g = \mathrm{d}r^2 + \mathrm{d}\theta^2$ and $F_0 = r\frac{\partial}{\partial \theta}$.

2.2.2 The vortex case ([15, 14])

In the vortex case one consider the punctured Euclidian space where the *vortex* is localized at the origin and the ship is a *passive tracer* in hydrodynamics whose motion is described by

$$\frac{\mathrm{d}x(t)}{\mathrm{d}t} = -\frac{ky(t)}{x(t)^2 + y(t)^2} + u_1(t)$$

$$\frac{\mathrm{d}y(t)}{\mathrm{d}t} = +\frac{ky(t)}{x(t)^2 + y(t)^2} + u_2(t),$$

where $k > 0$ is the *circulation parameter* and one has $F_1 = \frac{\partial}{\partial x}, F_2 = \frac{\partial}{\partial y}$ and $\|u\| \leq 1$. The problem is written in polar coordinates $x = r\cos\theta$, $y = r\sin\theta$ so that the Euclidian metric takes the form $g = \mathrm{d}r^2 + r^2\,\mathrm{d}\theta^2$ and the current transforms into $F_0 = \frac{k}{r^2}\frac{\partial}{\partial \theta}$. The ambient manifold is defined by $r \neq 0$, F_0 having a pole at the origin identified to $r = 0$.

2.2.3 Averaged Kepler case ([9])

The ambient space M is the *two-sphere of revolution*, the metric being defined $m^2(r) = \frac{\sin^2 r}{1 - \lambda \sin^2 r}$ where λ is an homotopy parameter deforming the *round sphere* if $\lambda = 0$ to the singular metric called *Grushin case* for $\lambda = 1$ and $\lambda = 4/5$ corresponds to the *averaged Kepler case,* where $e = \sin r$ is the eccentricty.

2.2.4 Ellipsoid of revolution ([27])

The ellipsoid is generated by the curve : $y = \sin\varphi$, $z = \varepsilon\cos\varphi$ where $0 < \varepsilon < 1$ corresponds to the *oblate* (flattened) case while $\varepsilon > 1$ corresponds to the *prolate* (elongated) case. The metric takes the form $g = F_1(\varphi)d\varphi^2 + F_2(\varphi)\,\mathrm{d}\theta^2$, with $F_1(\varphi) = \cos^2\varphi + \varepsilon^2\sin^2\varphi$, $F_2 = \sin^2\varphi$. The metric can be written in the normal form by setting $\mathrm{d}r = \sqrt{F_1(\varphi)}d\varphi$. This defines the metric on the two-sphere of revolution.

2.2.5 The Serret-Andoyer case ([12])

The Serret-Andoyer metric in the normal form is given by $m^2(r) = (Acn^2(\alpha r, k) + Bsn^2(\alpha r, k))^{-1}$, where cn and sn are Jacobi elliptic function so that $m(r)$ is periodic and moreover $m(r) = m(-r)$. One has $k^2 = \frac{B-A}{C-A}$, $\alpha = \sqrt{C-A}$, where $0 < A < B < C$ are parameters. This corresponds to a representation of the mechanical pendulum.

For the previous metrics, this defines Zermelo navigation problems associated to constant and linear current, on the covering space. In the ellipsoid case, the oblate case is different from the prolate case, in relation with permuting meridians and parallels and our study will cover only the oblate case. Note also that a two-sphere a constant current corresponds to a linear rotation with axis $0z$.

3 The geometric tools from optimal control theory and the Hamiltonian analysis

3.1 Generalities and Maximum Principle

If not mentioned, all the objects are in a smooth (C^∞ or C^ω) category. We consider a Zermelo navigation problem determined by a triplet (M, F_0, g) where M is a 2D-manifold with normal coordinates: $(q = (r, \theta))$,

$F_0(q)$ is a vector field defining the current (or wind) given by:

$$F_0 := \mu(r)\frac{\partial}{\partial\theta}$$

and where g is a metric of revolution in the form: $g = dr^2 + m^2(r)d\theta^2$. Taking $F_1 = \frac{\partial}{\partial r}$, $F_2 = \frac{1}{m(r)}\frac{\partial}{\partial\theta}$, from optimal control point of view, the Zermelo navigation problem is a time minimal transfer between two points (q_0, q_1) for the control system:

$$\dot{q} = F_0(q) + \sum_{i=1}^{2} u_i F_i, \quad u = (u_1, u_2) \quad \|u\| \le 1, \tag{2}$$

$u = (u_1, u_2)$ and the set of admissible controls $\mathcal{U}$ is the set of bounded measurable mapping defined on $[0, +\infty[$ and valued in the domain $U := \{u \,/\, \|u\| \le 1\}$. Fixing $q(0) = q_0$, we denote by $q(\cdot, q_0, u)$ the solution of (2) with $q(0) = q_0$, associated to $u(\cdot)$ and defined on a maximal interval J. We introduce the following:

Definition 3.1. *The fixed extremity mapping is the map $E^{q_0,t_f} : u(\cdot) \mapsto q(t_f, q_0, u(\cdot))$ and the extremity mapping is the map $E^{q_0} : u(\cdot) \mapsto q(\cdot, q_0, u(\cdot))$. The set of inputs being defined on a subdomain of L^∞. The time accessibility set $A(q_0, t_f)$ is the image of E^{q_0,t_f} and the accessibility set $A(q_0) = \bigcup_{t_f} A(q_0, t_f)$ is the image of the extremity mapping.*

Maximum Principle. We recall the maximum principle from [37] to parameterize the minimizers.

Proposition 3.1. *Let $H_i = p \cdot F_i(q)$ be the Hamiltonian lift of $F_i(q)$ for $i = 0, 1, 2$ and $H(q, p, u) = H_0(q, p) + \sum_{i=1}^{2} u_i H_i(q, p)$ denote the Hamiltonian lift of the system called pseudo-Hamiltonian. If $q(\cdot, u)$ are candidates as minimizers, there exists an absolutely continuous function $p(\cdot)$ (with $p(t) \neq 0$) such that (q, p, u) is solution of:*

$$\dot{q} = \frac{\partial H}{\partial p}, \quad \dot{p}(t) = -\frac{\partial H}{\partial q},$$
$$H(q, p, u) = \max_{\|v\| \le 1} H(q, p, v), \tag{3}$$

Moreover, the cost extended Hamiltonian $\mathbf{M}(q, p, u) = H(q, p, u) + p^0$ is such that p^0 is constant and ≤ 0. While $p^0 \ge 0$ corresponds to time maximizing solutions. Solving (3) leads to the following formulation

Proposition 3.2. *Denote by $\mathbf{M}(z)$, $z = (q, p)$, the maximized Hamiltonian $\mathbf{M}(z) = \max_{\|v\| \le 1} H(z, v)$, one has*

- *The maximizing controls are given by*

$$u_i(z) = \frac{H_i}{\sqrt{H_1^2 + H_2^2}}, \quad i = 1, 2. \tag{4}$$

- *The maximized Hamiltonian is given by*

$$\mathbf{M}(z) = H_0(z) + \sqrt{H_1^2 + H_2^2} + p^0 \tag{5}$$

  where p^0 is a constant and $p^0 \le 0$ in the time minimizing case and $p^0 \ge 0$ in the time maximizing case.

- *Candidates as time minimizers or maximizers are solutions of the Hamiltonian dynamics:*

$$\dot{z}(t) = \overrightarrow{\mathbf{M}}(z(t)), \tag{6}$$

  with

$$\overrightarrow{\mathbf{M}} = \frac{\partial \mathbf{M}}{\partial p}\frac{\partial}{\partial q} - \frac{\partial \mathbf{M}}{\partial q}\frac{\partial}{\partial p}$$

Definition 3.2. *An extremal is a solution $z(\cdot) = (q(\cdot), p(\cdot))$ of (6) and a projection of an extremal is called a* geodesic. *A geodesic is called* regular *if $t \mapsto q(t)$ is a one-to-one immersion. It is called* strict *if p is unique up to a factor,* normal *if $p^0 \neq 0$ and* abnormal *(or exceptional) if $p^0 = 0$. In the normal case it is called* hyperbolic *(resp. elliptic) if $p^0 < 0$ (resp. $p^0 > 0$).*

One has the following (see [17])

Proposition 3.3. *Let $z(\cdot) = (q(\cdot), p(\cdot))$ be a reference extremal defined on $[0, T]$ associated to u. If we endow the set of controls (valued in $\|u\| = 1$) with the L^∞-norm topology we have:*

1. *In the normal case, u is a singularity of the fixed time extremity mapping, that is the image of the Fréchet derivative is not of maximal rank.*

2. *In the abnormal case, u is a singularity of the extremity mapping.*

Definition 3.3. *Fixing $q(0) = q_0$, the exponential mapping is the map $(t, p(0)) \mapsto \Pi(exp\, t\overrightarrow{\mathbf{M}}(z(t)))$ where $\Pi : (q, p) \mapsto q$ is the q-projection. Take a regular normal geodesic $q(\cdot)$, a conjugate point along $q(\cdot)$ is a point where the exponential mapping is not an immersion and taking all such geodesics, the set of* first *conjugate points will form the* conjugate locus $C(q_0)$. *Given a geodesic, the* cut point *is the first point where it loses optimality and they will form the* cut locus $\Sigma(q_0)$. *The* separating line $L(q_0)$ *is the set of points where two minimizing geodesics starting from q_0 are intersecting.*

Computation of minimizers can be carried out using the maximized or non maximized Hamiltonian. We introduce the following.

3.2 Carathéodory-Zermelo-Goh transformation and evaluation of the accessibility set

3.2.1 Carathéodory-Zermelo-Goh (CZG) transformation

In the historical example [22], the authors integrated the dynamics of the heading angle α to parameterize the geodesics. This corresponds to the Goh transformation in optimal control and this will be crucial in our analysis.

Definition 3.4. *Consider the control system* (2), *with $q = (r, \theta)$ and u restricted to the unit sphere i.e $\|u\| = 1$. One can set $u = (\cos \alpha, \sin \alpha)$, α being the heading angle of the ship. Denote $\tilde{q} = (q, \alpha)$, $X(\tilde{q}) = F_0(q) + \cos \alpha\, F_1(q) + \sin \alpha\, F_2(q)$ and $Y(\tilde{q}) = \frac{\partial}{\partial \alpha}$. This leads to prolongate* (4) *into the* single-input affine system*:*

$$\dot{\tilde{q}} = X(\tilde{q}) + v\, Y(\tilde{q}) \tag{7}$$

where the derivative of the heading angle $v = \dot{\alpha}$ is the accessory control *and such tranformation is called Carathéodory-Zermelo-Goh transformation.*

The first consequence is the important geometric point of view presented next.

3.2.2 Evaluation of the extremity mapping and conjugate point computation in the regular case

We shall make use of the results of [17] proved in a n-dimensional setting, for single input systems, to calculate conjugate point in the normal and abnormal case for regular curves. It is based on the concepts of normal forms, important also in our study. Consider system (7), with coordinates $\tilde{z} = (q, \alpha, p, p_\alpha)$, p adjoint vector associated to q and p_α associated to α. This leads to introduce the extended Hamiltonian:

$$\tilde{H}(\tilde{z}, v) = \tilde{p} \cdot (X(\tilde{q}) + v\, Y(\tilde{q})), \quad \text{with} \quad v \in \mathbb{R}. \tag{8}$$

From [17], using the Maximum Principle in this setting we obtain the following parameterization of the geodesic curves. Let γ be a reference geodesic for the extended system defined on $[0, T]$. We assume the following :

(A1) The q-projection of γ is regular, and hence along γ, X and Y are independent.

(A2) The reference geodesic is strict and hence along γ, Y and $[X, Y]$ are linearly independent.

(A3) For the computation of (4), the generalized Legendre-Clebsch condition is satisfied along γ, i.e : $[[Y, X], Y] \notin \text{Span}\{Y, [Y, X]\}$.

Let us introduce the following determinants

$$D = \det(Y, [Y, X], [[Y, X], Y]),$$
$$D' = \det(Y, [Y, X], [[Y, X], X]), \qquad (9)$$
$$D'' = \det(Y, [Y, X], X),$$

and the following vector field called the CZG-geodesic field:

$$X_s = X + v_s Y \qquad (10)$$

where v_s is the feedback

$$v_s = -\frac{D'(\tilde{q})}{D(\tilde{q})}, \qquad (11)$$

and also the Jacobi (or variational equations)

$$\dot{\widehat{\delta \tilde{q}}}(t) = \frac{\partial X_s}{\partial \tilde{q}}(\tilde{q}(t)) \cdot \delta \tilde{q}, \qquad (12)$$

then, we have.

Theorem 3.1. *The geodesics under the CZG transformation extend into solutions of X_s. Moreover*

- *hyperbolic geodesics are in $DD'' > 0$,*

- *elliptic geodesics are in $DD'' < 0$,*

- *abnormal (or exceptional) geodesics are located in $D'' = 0$.*

Given a normal (hyperbolic or elliptic) geodesic defined on $[0, T]$ and let t_{1c} be the first associated conjugate time on $]0, T[$ i.e the first time for which the solution $J(t)$ of the Jacobi equation with $J(0) = Y(\tilde{q}(0))$ is such that $\det(J(t_{1c}), Y(\tilde{q}(t_1 c)), X(\tilde{q}(t_{1c})) = 0$. Abnormal geodesics are C^1-time minimizing and maximizing up to the first conjugate time t_{1c}, hyperbolic (resp. elliptic) geodesics are C^1-time minimizing (resp. maximizing).

This result is proved in [17] but we sketch the main step of the proof to understand the geometric construction.

Sketch of the proof. The main tool is to construct a semi-normal form for a reference geodesic satisfying our assumption for the feedback group. The reference geodesic denoted $\gamma(t)$ and defined on $[0, T]$ is identified to $t \mapsto (t, 0, 0)$ jet-space and the reference control can be taken as $v \equiv 0$, using a proper feedback. Normalization are obtained in the jet-space of $[X, Y]$ in the neighborhood of γ. We must distinguish normal and abnormal case.

Normal case. We can choose coordinates $\tilde{q} = (q_1, q_2, q_3)$ such that the system takes the form:

$$X = \left(1 + \sum_{i,j=2}^{3} a_{i,j}(q_1) q_i q_j\right) \frac{\partial}{\partial q_1} + q_3 \frac{\partial}{\partial q_2} + \varepsilon_1,$$
$$Y = \frac{\partial}{\partial q_3}, \qquad (13)$$

with $a_{33} < 0$ (resp. $a_{33} > 0$) in the hyperbolic (resp. elliptic) case.

Abnormal Case We can choose coordinates $\tilde{q} = (q_1, q_2, q_3)$ such that the system takes the form:

$$X = (1 + q_2) \frac{\partial}{\partial q_1} + \frac{1}{2} a(q_1) q_2^2 \frac{\partial}{\partial q_3} + \varepsilon_2,$$
$$Y = \frac{\partial}{\partial q_2}. \qquad (14)$$

See [17] for details of the computation and description of ε_1, ε_2. Taking $\varepsilon_i = 0$ and $q_1 = t$ in (13)-(14), one can evaluate the accessibility set and it boundaries, filled by geodesics, and compute conjugate points and deducing the optimality status. One has:

Optimality status in normal case. Using the normalization in (13) one sets: $q_1(t) = t + w_1(t)$ and projection of the accessibility set in w_1-direction is represented on Fig. 1. Note that hyperbolic and elliptic geodesics amount respectively to minimize and maximize the w_1-coordinate. If $t > t_{1c}$ (first conjugate time) the fixed extremity mapping becomes open.
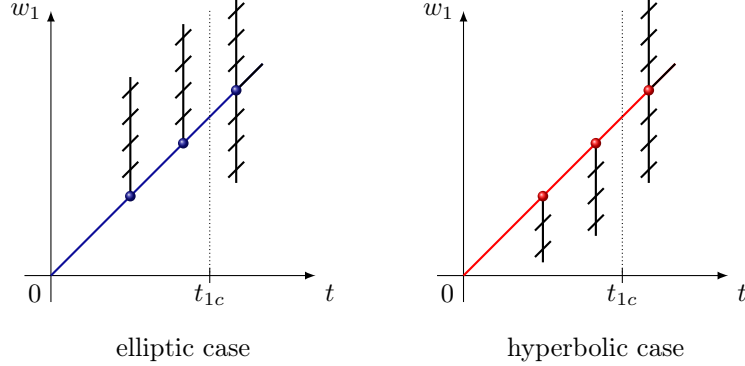

Figure 1: Projection of the fixed time accessibility set on the w_1-coordinate; t_{1c} bieng the first conjugate time.

Optimality status in abnormal case. In this case, one must evaluate the *time evolution* of the accessibility set and it boundaries. It is represented on Fig. 2. The reference geodesic is $\gamma\colon t \mapsto (t, 0, 0)$ and is associated to $v \equiv 0$. We fix t along the reference curve and let a time t_f in a neighborhood of t. Using the model, we compute geodesics such that :

$$q_1(t_f) = t, \quad q_2(t_f) = 0, \tag{15}$$

and the associated cost is given by

$$q_3(t_f) = \int_0^{t_f} a(q_1)q_2^2 \, \mathrm{d}t. \tag{16}$$

This give the parameterization of the boundaries of the accessibility set as:

$$q_3(t_f) = \alpha(t - t_f)^2 + o(t - t_f)^3 \tag{17}$$

α being a positive invariant, given by the Jacobi equation. Note that the model (14) clearly shows that the abnormal curve is a so-called limit curve, as observed by Carathéodory [22]. It's also show that conjugate points cannot occur in the 3d-case, see again [17] for the occurence of conjugate points along abnormal curve in the n-dimensional case for $n > 3$. In this analysis, the integrability of the geodesic flow is not required but in the model, the accessibility set can nevertheless be evaluated since in the models, the extremity mapping can be computed (making $\varepsilon_i = 0$).
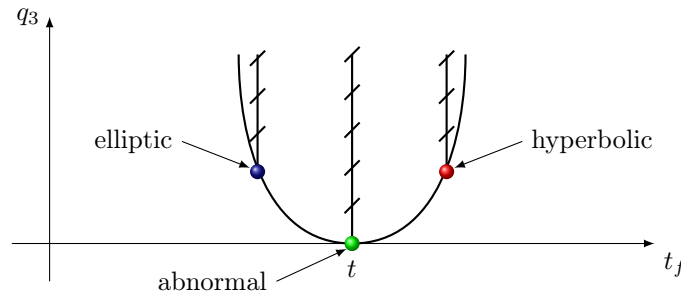

Figure 2: Projection of the accessibility sets on the q_3-coordinate in the abnormal case.

$\square$

Next, the CZG tranformation is used to integrate by quadrature the geodesic flow in the rotational case. Moreover, a clear geometric integration is performed clarifying the integration process in the historical example.

3.2.3 The geometric frame and the integrability properties

Geometric frame Using the CZG extension and $\tilde{q} = (r, \theta, \alpha)$ the coordinates, we have:

$$X = \cos\alpha \frac{\partial}{\partial r} + \left(\mu(r) + \frac{\sin\alpha}{m(r)}\right)\frac{\partial}{\partial\theta}.$$

and Lie bracket computation gives:

$$[Y, X](\tilde{q}) \qquad = \sin\alpha \frac{\partial}{\partial r} - \frac{\cos\alpha}{m(r)}\frac{\partial}{\partial\theta},$$

$$[[Y, X], Y](\tilde{q}) = \cos\alpha \frac{\partial}{\partial r} + \frac{\sin\alpha}{m(r)}\frac{\partial}{\partial\theta},$$

$$[[Y, X], X](\tilde{q}) = \left(-\mu'(r)\sin\alpha + \frac{m'(r)}{m^2(r)}\right)\frac{\partial}{\partial\theta}.$$

Hence we have:

$$D(\tilde{q}) = \frac{1}{m(r)},$$

$$D'(\tilde{q}) = -\mu'(r)\sin^2\alpha + \frac{m'(r)\sin\alpha}{m^2(r)},$$

$$D''(\tilde{q}) = \mu(r)\sin\alpha + \frac{1}{m(r)}.$$

So that by construction, conditions $(A2)$ and $(A3)$ are satisfied, but the collinearity condition $(A1)$ can be violated and we have

Lemma 3.1. *The collinearity condition (A_1) can be violated only along the abnormal curves at points where:*

$$\cos\alpha = \mu(r) + \frac{\sin\alpha}{m(r)} = 0.$$

The dynamics is given by

$$\dot{r} = \cos\alpha,$$

$$\dot{\theta} = \mu(r) + \frac{\sin\alpha}{m(r)}, \qquad (18)$$

$$\dot{\alpha} = \mu'(r)m(r)\sin^2\alpha - \frac{m'(r)\sin\alpha}{m(r)}.$$

and we have the following.

Proposition 3.4. *The dynamics (18) can be integrated by quadrature.*

Proof. The pseudo-Hamiltonian takes the form:

$$H = p_r\cos\alpha + p_\theta\left(\mu(r) + \frac{\sin\alpha}{m(r)}\right) + p^0. \qquad (19)$$

Moreover, from the maximization condition one has:

$$\frac{\partial H}{\partial\alpha} = 0,$$

which gives the *Clairaut relation*:

$$p_r\sin\alpha = \frac{p_\theta}{m(r)}\cos\alpha.$$

So, $(p_r, p_\theta/m(r))$ and $(\cos\alpha, \sin\alpha)$ are parallels and thanks to this, one has $(p_r, p_\theta/m(r)) = \lambda(\cos\alpha, \sin\alpha)$, with $\lambda = \left(p_r^2 + \frac{p_\theta^2}{m^2(r)}\right)^{1/2}$. Plugging such p_r into (19) allows us to define the following implicit relation between α and r:

$$p_\theta\left(\mu(r) + \frac{1}{m(r)\sin\alpha}\right) + p^0 = 0. \qquad (20)$$

for $\alpha \neq 0$ $[\pi]$. By homogeneity one can fix $\lambda(0) = 1$ and have $(p_{r_0}, p_\theta/m(r_0)) = (\cos \alpha_0, \sin \alpha_0)$. So that, one gets $p_\theta = m(r_0) \sin \alpha$ and from the maximized Hamiltonian one deduces $p^0 = -1 - p_\theta \mu(r_0)$.

Equation (18) can be solved by quadrature. From geometric control point of view, it amounts to compute first the control using the integration of the heading angle, r being given by equation (20). Then, θ can be obtained using a further quadrature. In the case where $\alpha_0 = 0$ $[\pi]$, one has:

$$\alpha = \alpha_0, \quad r(t) = \pm t + r_0, \quad \text{and} \quad \theta(t) = \int_0^t \mu(r) \, dt.$$

$\square$

One further consequence bieng the parameterization of the conjugate locus.

3.2.4 Parameterization of the conjugate locus in the normal case

Conjugate points are given using theorem 3.1 by the condition

$$det(J(t_{1c}), Y(\tilde{q}(t_{1c})), X(\tilde{q}(t_{1c}))) = 0$$

where $J(t)$ denotes the Jacobi field which is semi-vertical at $t = 0$, i.e $J(0) = Y(\tilde{q}(0))$. Using the *ad-formula*, one has:

$$J(t) = e^{t \, adX_s}(Y(\tilde{q}(t)) = \sum_{n \geq 0} \frac{t^n}{n!} ad^n X_s(Y)(\tilde{q}(t)) \tag{21}$$

where $adX_s \cdot Y = [X_s, Y]$ denotes the adjoint operator. Since $\tilde{q}(t)$ is a geodesic curve one has

$$J(t) \in Span\{Y(\tilde{q}(t)), [Y, X_s](\tilde{q}(t))\}$$

and it can be written as

$$J(t) = \lambda_1(t) Y(\tilde{q}(t)) + \lambda_2(t)[Y, X_s](\tilde{q}(t)),$$

so conjugate times t_c (in particular the first conjugate time t_{1c}) are given by $\lambda_2(t_c) = 0$ i.e $J(t)$ collinear to $Y(\tilde{q}(t))$. Thus we have:

Proposition 3.5. *In the rotational Zermelo navigation problem, the conjugate locus is defined by the Jacobi field $J(t)$ which can be integrated thanks to the integrability property of the dynamics and we have: $J(t)$ belongs to the kernel of the* Cartan-Hilbert *form ω defined by:*

$$\omega(X_s) = 1, \quad \omega(Y) = \omega([Y, X_s]) = 0,$$

and at the conjugate time t_c, $J(t_c)$ is semi-vertical i.e collinear to $Y(\tilde{q}(t_c))$.

This defined the conjugate locus in the normal case. Moreover, note that the semi-normal form (13) defines a canonical form of Jacobi equation in the general frame of single-input affine systems, this gives the singularity of the time value mapping associated to conjugate points in the normal case.

3.2.5 Historical example as a model of the cusp singularity in the abnormal case

We can refer to [14] for a complete presentation. Recall first that for a Zermelo navigation problem the domain in the (r, θ) coordinates is split into bord $r_0 < r < r_1$ where, if $q = (r, \theta)$ is such that $\|F_0\|_g < 1$ (resp. $\|F_0\|_g > 1$) the current is called weak (resp. strong). Transition between the two case being a moderate current where $\|F_0\|_g = 1$. In the weak case, there is no abnormal geodesics. In the strong case there is two abnormal derections defined by two distinct heading angles denoted $\{\alpha_1, \alpha_2\}$ and they form the tangent to the indicatrix defined by: $F_0(q) + \|u\|$ where u is given by $u = (\cos \alpha, \sin \alpha)$. We consider the following coordinates $\tilde{q} = (x, y, \gamma) = (\theta, r, \pi/2 - \alpha)$, where r, θ and α are understood in the sense of the previous section. It's interesting to use the historical example of Caratheodory-Zermelo as a model (normal form) to make the following analysis. We get the following, illustrated on figures 3-4 (see [22] for more details): The two abnormal directions at the initial point are given by

$$\gamma_a^1 = \arccos\left(-\frac{1}{y_0}\right) \quad \text{and} \quad \gamma_a^2 = -\arccos\left(-\frac{1}{y_0}\right).$$

A cusp point denoted $(x_{\text{cusp}}, y_{\text{cusp}}, \gamma_{\text{cusp}})$ occurs along an abnormal geodesic at time t_{cusp} when $\dot{x}(t_{\text{cusp}}) = \dot{y}(t_{\text{cusp}}) = 0$. This gives

$$t_{\text{cusp}} = \tan\gamma_0, \quad \gamma_{\text{cusp}} = 0 \ [\pi] \ \text{ and } \ y_{\text{cusp}} = \text{sign}(y_0).$$

Finally, x_{cusp} is deduced from the analytical expressions given above. And we deduce:

- The abnormal geodesic with the cusp singularity is the limit curve of the micro-local sector, formed by self-intersecting hyperbolic geodesics.

- The abnormal geodesic is optimal up to the cusp point. Hence it corresponds to a concept of conjugate point along the *nonsmooth* abnormal geodesic.

- Moreover, due to the loss of local accessibility associated to the limit geodesic, the time minimal value function is *not continuous*. This is clear from Fig. 4. To reach from the initial point q_0 a point B at right of the limit curve, one must use a self-intersecting normal geodesic so that at the intersection with the abnormal geodesic, the time is longer along the normal than along the abnormal geodesic. We also observe that in this sector, the normal geodesic is optimal up to the intersection point with the abnormal geodesic.
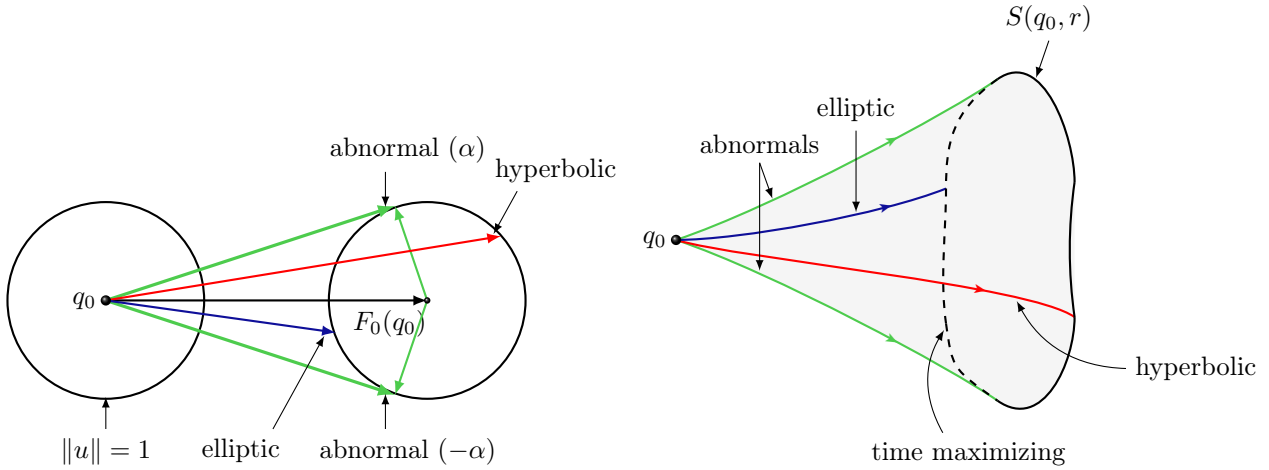

Figure 3: (Left) ball of directions, (Right) Small sphere and ball in the strong current case. (F_0 parallel direction)

3.2.6 Conclusion: models of conjugate points

Normal case. It is deduce using the CZG-representation by (13) where X_s can be set thanks to integrability as $X_s = \partial/\partial x$ and the accessory LQ problem from [17] can be set to ($q = (x, y, z)$):

$$1 + L(t, y, z)\frac{\partial}{\partial x} + z\frac{\partial}{\partial y} + u\frac{\partial}{\partial z}$$

where the reference geodesic is normalized to $t \mapsto (t, 0, 0)$ and the quadratic form L is given by

$$L(t, y, z) = a(t)z^2 + 2b(t)yz + c(t)y^2,$$

and $a < 0$ (resp. $a > 0$) in the hyperbolic (resp. elliptic) case. While a, b, c can be compute using Lie brackets along the reference geodesic. The associated Jacobi equation takes the form of the second order diffrential operator:

$$\frac{d^2\varphi}{dt^2} + \frac{da}{dt} + a^{-1}\frac{d\varphi}{dt} + \left(\frac{db}{dt} - c\right)a^{-1}\varphi = 0$$
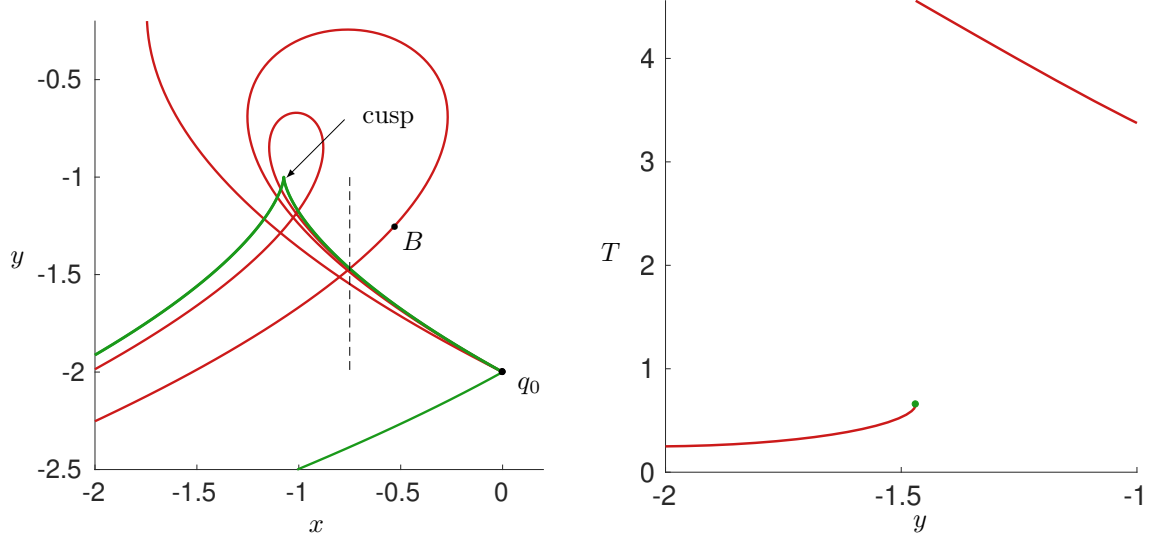
Figure 4: (Left) The initial point is $q_0 = (-2, 0)$. The abnormal geodesic with the cusp singularity is in green while the others geodesics in red are hyperbolic. We can see that the cusp singularity is the limit of self-intersecting hyperbolic geodesics. Besides, to reach the point B from q_0, one has to use a hyperbolic self-intersecting geodesic. When this hyperbolic geodesic intersects the abnormal, the time is longer along the hyperbolic than the abnormal. At this intersection, the hyperbolic geodesic ceases to be optimal. (Right) The time minimal value function along the dashed segment from the left subgraph. The discontinuity occurs at the intersection between the hyperbolic and abnormal geodesics. It is represented by the green dot, which is the time along the abnormal geodesic.

If we set $A = \frac{da}{dt} a^{-1}$, $B = \left(\frac{db}{dt} - c\right) a^{-1}$, $C = exp \int_0^t -\frac{A(s)}{2} ds$ and $K = \frac{d^2 C}{dt^2} + A \frac{dC}{dt} + BC$, this equation can be set in the canonical form

$$\frac{d^2 J}{dt^2} + K(t) J = 0 \tag{22}$$

and by analogy with the Riemannian case, $K(t)$ is called the *curvature* of the Zermelo navigation problem.

Abnormal case. Conjugate point can be computed as a cusp singularity of the historical model described by (18) where $p^0 = 0$ (abnromal case) and using Lie brackets only with the relation $D'' = 0$ and $A = (0.0, 1.5)$ initial point gives the reference abnormal arc. We get the following figure 5 summarizing the two cases excerpted from geodesic beheviors only.

Figure 5: Conjugate points in the 2D-space

3.3 The mechanical representation and Hamiltonian dynamics anlysis. The generalized Morse-Reeb classification. Micro-local analysis

Definition 3.5. *Let $\frac{\mathrm{d}x}{\mathrm{d}t} = X(x)$ be a smooth dynamical system and we may assume that the vector field X is complete. We denote by $x(t, x_0)$ the solution emanating from x_0 at $t = 0$. A point x_1 is called a ω- limit point (resp. $\alpha-$ limit point) if there exists an increasing sequence $0 < t_1 < \cdots < t_n, t_n \to +\infty$ (resp. a decreasing sequence $0 > t_1 > ... < t_n, t_n \to -\infty$) such that $x_1 = \lim_{t_n \to +\infty} x(t, x_0)$ (resp. $x_1 = \lim_{t_n \to -\infty} x(t, x_0)$). Taking all such points, they will define the $\omega - limit$ set $\Lambda^+(x_0)$ (resp. the $\alpha - limit$ set $\Lambda^-(x_0)$).*

Theorem 3.2 (Liouville-Arnold). *Let $\mathbf{H}$ be an Hamiltonian vector field on T^*M (M being 2-dimensional) with an additional first integral G so that $\{H, G\} = 0$. Assume the corresponding vector field are complete and moreover H and G are functionally independant. Then the hamiltonian vector field is called* Liouville-integrable *and moreover if the set T_ξ defined by $[H = c_1, G = c_2; \xi = (c_1, c_2)\}$ is regular. Then we have.*

1. *T_ξ is a smooth manifold invariant by the flow of $\mathbf{H}$ and $\mathbf{G}$.*

2. *If T_ξ is connected and compact, then T_ξ is diffeomorphic to the 2-dimensional torus T^2 and it is called a* Liouville torus.

3. *The Liouville foliation is trivial that is in some neighborhood of the torus T_ξ being a direct product of T^2 and the disc D^2.*

4. *In the neighborhood of $U = T^2 \times D^2$ there exist* action-angle variables *so that the dynamics can be written : $\frac{\mathrm{d}s_i}{\mathrm{d}t} = 0, \frac{d\varphi_i}{\mathrm{d}t} = \alpha_i(s_1, s_2), i = 1, 2$.*

Application to the averaged Kepler case. In this case the ambient manifold M is the (compact) 2-dimensional sphere. If g is the metric in normal coordinates the hamiltonian vector field is defined by $H = \frac{1}{2}(p_r^2 + \frac{p_\theta^2}{m^2(r)})$ and $G = p_\theta$ is the additional (linear) first integral. Trajectories of $\mathbf{H}$ splits into three cases : the meridians defined by θ constant, the equator which can be identified to $\pi/2$ with $r \in [0, \pi]$ in the normal coordinates on the sphere. All the other trajectories are formed by solutions so that r oscillates periodically of the mechanical system

$$\left(\frac{\mathrm{d}r}{\mathrm{d}t}\right)^2 = 1 - V(r, p_\theta) = G(r, p_\theta),$$

which can be integrated starting from the equator $r_0 = \pi/2$ and using by example the ascending branch, the term $V = \frac{p_\theta^2}{m^2(r)}$ being the *potential*. One further integration is necessary in order to recover the $\theta-$variable using the hamiltonian dynamics. Parameterizing by r on each branch this dynamics takes the form

$$\frac{\mathrm{d}\theta}{\mathrm{d}r} = \frac{1}{\sqrt{G(r, p_\theta)}} \frac{\partial H}{\partial p_\theta}.$$

This allows to compute the variation denoted $\Delta\theta/2$ of the angle θ starting from the equator and on the ascending branch the total variation to return to the equator being $\Delta\theta$. Note that in the limit case of the equator the rotation is stationary since r is constant. This gives the complete description of the Liouville tori, with periodic trajectories if $\Delta\theta/2\pi$ *is rational* and dense orbits if $\Delta\theta/2\pi$ *is irrational.*

Theorem 3.3. *Given a Zermelo navigation problem on a surface of revolution, with parallel current.*

1. *Denoting $\|p\|_g = \left(p_{r_0}^2 + \frac{p_\theta^2}{m^2(r_0)}\right)^{1/2}$, the evolution of the in the (r, p_r) space is decribed by the hamiltonian dynamics*

$$\frac{\mathrm{d}r}{\mathrm{d}t} = \frac{p_r}{\|p\|_g}, \qquad \frac{dp_r}{\mathrm{d}t} = -p_\theta \mu'(r) + \frac{p_\theta^2 m'(r)}{m^3(r)\|p\|_g}.$$

2. *It can be integrated using the mechanical system representation*

$$\left(\frac{\mathrm{d}r}{\mathrm{d}t}\right)^2 + V_\epsilon(r, p_\theta) = 1$$

13

where the generalized potential *is given by*

$$V_\epsilon(r, p\theta) = \frac{p_\theta^2}{m^2(r)(\varepsilon + p_\theta \mu(r))^2},$$

where $\varepsilon = -p^0 < 0, = 0, > 0$ corespond respectively to the hyperbolic, elliptic and abnormal case.

3. *Since the hamiltonian is constant we normalize $\|p(0)\|_g = 1$, i.e $(\varepsilon + p_\theta \mu(r_0)) = -1$, one has:*

$$p_r^2 = (\varepsilon + p_\theta \mu(r_0))^2 - \frac{p_\theta^2}{m^2(r)}$$

with

$$p_\theta \in J(r_0, p_{r_0}) = \{p_\theta \mid \|p(0)\|_g = 1\}.$$

Proof. The first point of theorem is a consequence of the Maximum Principle, in particular it comes from equation (3).

For the second and third points, we have on one side, from the Hamiltonian: $\|p\|_r = -\varepsilon - p_\theta \mu(r)$, so:

$$p_r^2 = \|p\|_r^2 - \frac{p_\theta^2}{m^2(r)} = (\varepsilon + p_\theta \mu(r))^2 - \frac{p_\theta^2}{m^2(r)}. \tag{23}$$

On other side, from the restricted system in (r, p_r) one has:

$$\dot{r} = \frac{p_r}{\|p\|_r}$$

$$\dot{p}_r = -p_\theta \mu'(r) + \frac{p_\theta^2 \, m'(r)}{m^3(r)\|p\|_r}.$$

So that, $\dot{r}^2 = \frac{p_r^2}{\|p\|_r^2}$. Finally, using these two relations, we deduce:

$$\begin{aligned}
\dot{r}^2 &= \frac{p_r^2}{\|p\|_r^2} \\
&= \frac{(\varepsilon + p_\theta \mu(r))^2 - \frac{p_\theta^2}{m^2(r)}}{(\varepsilon + p_\theta \mu(r))^2} \\
&= 1 - \frac{p_\theta^2}{m^2(r)\,(\varepsilon + p_\theta \mu(r))^2},
\end{aligned}$$

conclusion then follows. $\qquad\square$

Definition 3.6. *The classification of trajectories of the restricted hamiltonian dynamics, where p_θ is fixed is called the* Generalized-Morse-Reeb (GMR) *classification defined by the generalized potential V_ϵ.*

Definition 3.7. *Assume the hyperbolic case $\varepsilon < 0$. An equator $r = r_1$ is an equilibrium point $(r_1, 0)$ of the restricted dynamics. It is called $L - elliptic$ if the linearized dynamics is with spectrum $\{\pm i\alpha, \alpha \neq 0\}$, $L - hyperbolic$ if the spectrum is of the form $\{\lambda, -\lambda, \lambda \neq 0\}$ and $L - parabolic$ if the spectrum is zero. The elliptic case corresponding respectively to a stable case associated a minimum of the potential and in the hyperbolic case an unstable case associated to a maximum. An equator corresponding to a stationary rotation, it is called* positive rotation *(resp. negative) if θ is rotating with a positive (resp. negative) frequency. A separatrix geodesic is a geodesic $e(t) = (r(t), *)$ such that $r(t) \to r_1$ as $t \to \infty$ and it is contained in the same level of the Hamiltonian and this is called a singular level.*

Definition 3.8. *A generalized Reeb component is a separatrix solution $e(t) = (r(t), *)$ so that $r(t)$ converges respectively when $t \to \pm\infty$ to two equators solutions and with different orientations.*

Definition 3.9. *Let U be an adapted neighborhood of q_0. Geodesics at the initial time decompose into starting ascending branch, starting descending branch or tangential to the parallel for which one must consider the case with positive or negative acceleration $\frac{d^2 r}{dt^2}(0)$. Note that if we start from the equator both coincide. The* first return to the equator *(resp. the meridian) associated to a geodesic is the first point such that the geodesic reintersects the equator (resp meridian) passing through the initial point.*

Proposition 3.6. *Considering the hyperbolic case ($\varepsilon = -1$), couples (r, p_θ) forming by r-equators and parameterized p_θ of separatrices are solutions of the system:*

$$V_\varepsilon(r, p_\theta) = 1 \quad and \quad \frac{\partial V_\varepsilon}{\partial r}(r, p_\theta) = 0, \quad with \quad p_\theta \neq 0.$$

Proposition 3.7. *Let U be and adapted neighborhood of $q_0 = (r_0, \theta_0)$. Levels sets sin the GMR-classification splits into compact levels corresponding to $r - periodic$ geodesics and non-compact level sets corresponding to $r - aperiodic$ geodesics restricted to the neighbohood U. If r_1 is an equator which is $L - elliptic$, then locally the Liouville foliation by Liouville tori is preserved.*

Proposition 3.8. *Let q_0 be a fixed initial condition, then using the GMR-classification for each adapted neighborhood of q_0 one can stratified the set of geodesics emanating from q_0 into micro-local (conic) sectors corresponding to compact and non-compact geodesics.*

Remark 1. *The decomposition depens upon the adapted neighborhood and can be obtained using the potentiel retricted to the domain. One can easily have situations with two compact sectors separated by a singular level with a separatrix geodesic and an equator for which when retricting the domain, the singular level separates compact and non-compact orbits.*

Example 1. *In the averaged Kepler case, the mico-local classification at a point on the equator gives the following. Retricting to p_θ positive, one has the following decomposition. The meridian with $p_\theta = 0$ formed by the ascending and descending branches and correspond to non-compact orbit in the covering manifold M^c, the micro-sector formed by $p_\theta \in]0, m(\pi/2[$ where the level set is filled by the same periodic orbit corrresponding to different ascending and descending branches with $\pm p_r(0)$ and the equator corresponding to $p_\theta = m(\pi/2)$, where the two branches are similar and the level set is a single point.*

Example 2. *In the Serret-Andoyer case, starting from the equator identified to zero and corresponding to the stable position of the pendulum we have two sectors associated repectively to rotating and oscillating solutions of the pendulum, separated by the separatrices. The rotating solutions correspons to non compact orbits on the plane but periodic if they are interpreted on the cylinder. On this surface oscillating trajectories are homotopic to a point but not the rotating trajectories.*

4 Case studies

4.1 The Carathéodory-Zermelo historical example

In this presentation, all the details of the computations are not given, for a complete study of this example, based on the Carathéodory-Zermelo-Goh point of view, see [14]. Recall that, considering the following coordinates $\tilde{q} = (x, y, \gamma) = (\theta, r, \pi/2 - \alpha)$, where r, θ and α are understood in the sense of section 3, dynamics takes the form:

$$\dot{x} = y + \cos\gamma, \quad \dot{y} = \sin\gamma, \quad \dot{\gamma} = -\cos^2\gamma.$$

Straighforward computations using the previous section leads to

$$D(\tilde{q}) = 1, \quad D'(\tilde{q}) = \cos^2\gamma \quad and \quad D''(\tilde{q}) = y\cos\gamma + 1,$$

and thanks to Theorem 3.1 we can parameterize abnormal, hyperbolic and elliptic extremals.

- **Abnormal case.** The abnormal geodesics are contained in $D'' = y\cos\gamma + 1 = 0$. Hence, given an initial condition (x_0, y_0, γ_0) such that $|y_0| \geq 1$, the associated geodesic is abnormal if $\gamma_0 \in \{\gamma_a^1, \gamma_a^2\}$ with

$$\gamma_a^1 = \arccos\left(-\frac{1}{y_0}\right) \quad and \quad \gamma_a^2 = -\arccos\left(-\frac{1}{y_0}\right).$$

  If the current is strong, that is if $|y_0| > 1$, then $\gamma_a^1 \neq \gamma_a^2$ and we have two abnormals. Else, if $|y_0| = 1$ there is only one abnormal, and if $|y_0| < 1$ (this correspond to a weak current) there is no abnormals.

- **Normal case.** The hyperbolic (resp. elliptic) geodesics are contained in $DD'' = D'' > 0$ (resp. $DD'' = D'' < 0$). Hence, given an initial condition (x_0, y_0, γ_0):

- if $|y_0| < 1$, then $y_0 \cos \gamma_0 + 1 > 0$ and thus the corresponding geodesic is hyperbolic.
- for $|y_0| = 1$, if the geodesic is normal, then it is hyperbolic.
- for $|y_0| > 1$, if the geodesic is normal, then it is either hyperbolic or elliptic depending on the sign of $y_0 \cos \gamma_0 + 1$. Note that the hyperbolic and elliptic geodesics are separated by the abnormal geodesics as illustrated in Fig. 3.

To complete the discussion about the historical example, we give the integration of the system.

Proposition 4.1. *Let (x_0, y_0, γ_0) be the initial condition, the corresponding solution $(x(t), y(t), \gamma(t))$ is given as follows.*

- *For $\gamma_0 = \pm\pi/2$ one has:*

$$\gamma(t) = \gamma_0, \quad y(t) = \pm t + y_0 \quad and \quad x(t) = \pm \frac{t^2}{2} + y_0 t + x_0.$$

- *For $\gamma_0 \in (-\pi/2, \pi/2)$, one has:*

$$\gamma(t) = \mathrm{atan}\,(\tan \gamma_0 - t), \quad y(t) = y_0 + \frac{1}{\cos \gamma_0} - \frac{1}{\cos \gamma(t)},$$

$$x(t) = \frac{1}{2} \left[\ln \left| \frac{\cos \gamma}{1 + \sin \gamma} \right| \right]_{\gamma_0}^{\gamma(t)} + \frac{1}{2} \left[\frac{\tan \gamma}{\cos \gamma} \right]_{\gamma_0}^{\gamma(t)} + \left(y_0 + \frac{1}{\cos \gamma_0} \right) t + x_0.$$

- *For $\gamma_0 \in (-\pi, -\pi/2) \cup (\pi/2, \pi]$, one has:*

$$\gamma(t) = \pi + \mathrm{atan}\,(\tan \gamma_0 - t), \quad y(t) = y_0 + \frac{1}{\cos \gamma_0} - \frac{1}{\cos \gamma(t)},$$

$$x(t) = \frac{1}{2} \left[\ln \left| \frac{\cos \gamma}{1 + \sin \gamma} \right| \right]_{\gamma_0}^{\gamma(t)} + \frac{1}{2} \left[\frac{\tan \gamma}{\cos \gamma} \right]_{\gamma_0}^{\gamma(t)} + \left(y_0 + \frac{1}{\cos \gamma_0} \right) t + x_0.$$

Synthesis: Cusp singularity and regularity of the value function. We use the heading angle and the Clairaut relation to stratified the Lagragian manifold $\mathcal{L} = \exp t\mathbf{M}(q_0)$, where q_0 is in the strong current domain (see Figs. 6 and 7). One can also compute the time minimal synthesis. In the strong current case, q_0 is not strongly locally controllable, i.e $A(q_0, t)$ is not a neighborhood of q_0 for small time. The time $T(q_0)$ along the loop is the limit time such that $A(q_0, t)$ is a neighborhood of q_0.

Denote by $\Sigma(q_0)$ the adherence of the cut locus for geodesics starting at q_0 and contained in the adapted neighborhood one has:

Proposition 4.2. *Let q_0 in a strong current domain, then:*

1. *For $t > T(q_0)$, $A(q_0, t)$ is a neighborhood of q_0.*

2. *$\Sigma(q_0)$ is the abnormal curve up to the cusp point, corresponding to a conjugate point along the abnormal curve.*

4.2 The Averaged Kepler case

4.2.1 Riemannian case

One takes

$$m_\lambda^2(\varphi) = \frac{\sin^2 \varphi}{(1 - \lambda \sin^2 \varphi)}$$

Where $\lambda \in (0, 1)$ is an homotopy parameter, $\lambda = 0$ being the round sphere, $\lambda = 1$ is the Grushin case, with a singularity at the equator while $\lambda = 4/5$ is associated to Kepler orbit transfers. The Gauss curvature is

$$K_\lambda = \frac{1}{(1 - \lambda \sin^2 \varphi)} ((1 - \lambda) - 2\lambda \cos^2 \varphi).$$
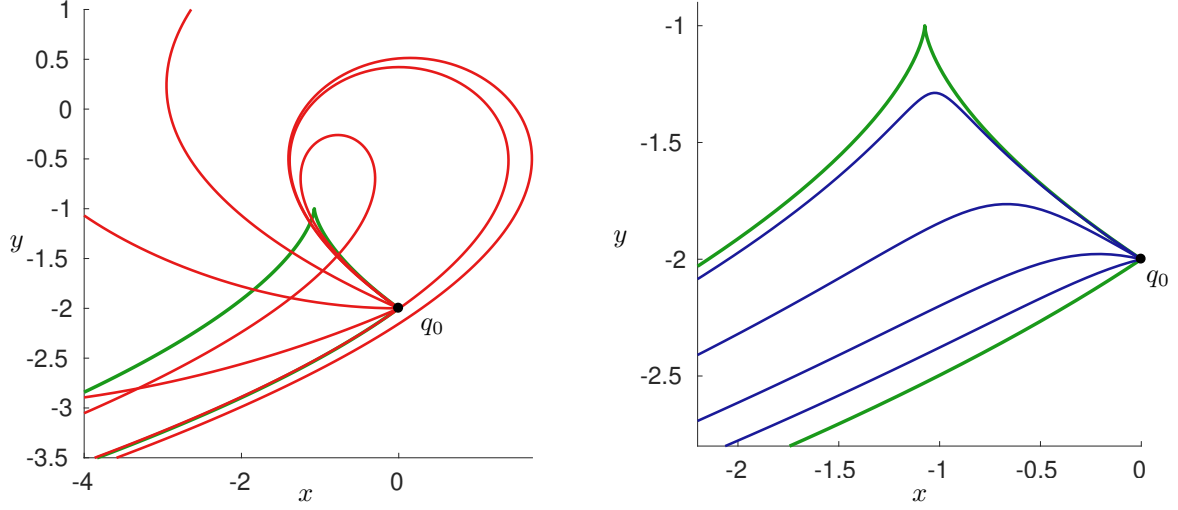
Figure 6: (Left) We display (in red) hyperbolic geodesics that started from the initial point $q_0 = (-2, 0)$ portrayed in black, in the whole conic neighborhood delimited by the two abnormals (in green). (Right) We display (in blue) elliptic geodesics from the same initial point and with the same sector.
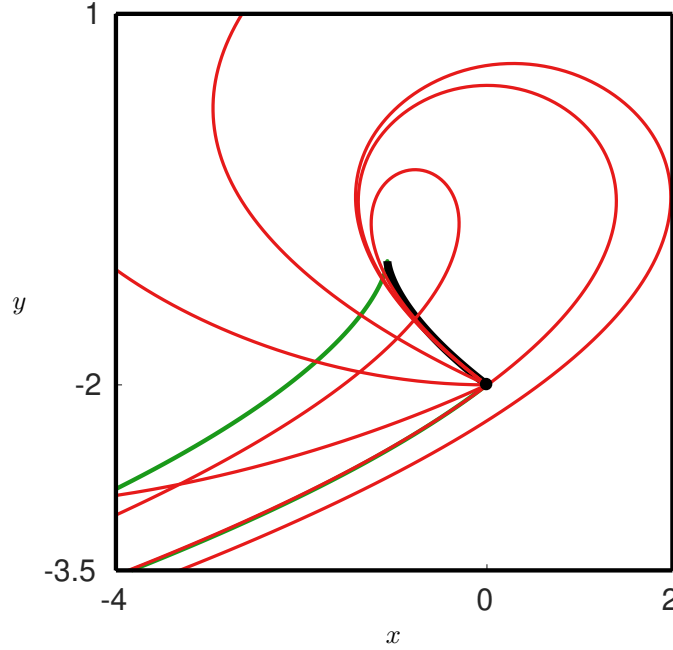

Figure 7: Minimal time optimal synthesis in an adapted rectangle neighborhood containing the limit loop. The initial point is $q_0 = (-2, 0)$. The abnormal geodesics are represented in green and in red are represented hyperbolic geodesics. The cut locus, form by the abnormal with a cusp, up to this cusp, is shown in thick black along.

The equator is $\varphi = \pi/2$ and we introduce $r := \pi/2 - \varphi$ to normalize the equator to zero and it is the only parallel solution. The metric is taken in the normal form $g = \mathrm{d}r^2 + m^2(r)\,\mathrm{d}\theta^2$ where we use the notation $r = \pi - \varphi$. One set $m_\lambda(r) = m_\lambda(\pi - \varphi)$ and the metric is reflectionally symmetric with respect to the equator, that is $m(r) = m(-r)$, which is crucial for the explicit determination of the conjugate and cut loci. Using the Hamiltonian formalism, we associate to the metric the Hamiltonian

$$H = \frac{1}{2}\left(p_r^2 + \frac{p_\theta^2}{m(r)}\right)$$

17

and parameterizing by arc-length amounts to set $H = 1/2$. To integrate the geodesisc leads to introduce the characteristic equation

$$\left(\frac{dr}{dt}\right)^2 + V(r, p_\theta) = 1, \quad \text{with} \quad V(r, p_\theta) = \frac{p_\theta^2}{m(r)}.$$

A geodesic is either a meridian, the equator or each other solution is such that r is periodic and oscillates between $-r_+$ and r_+ and is entirely determined by a branch of the characteristic equation evaluated on the quarter of period $T/4$ where $r(t)$ belongs to $[0, r_+]$, r_+ being the posive root of the equation $V = 1$, the period being given by the integral

$$\frac{T}{4} = \int_0^{r_+} \frac{dr}{(1 - V(r, p_\theta))^{1/2}},$$

which depends upon p_θ. By symmetry with respect to the meridian it can be supposed non negative and belonging to $]0, \mathrm{m}(0)[$. To make the analysis we introduce the application called the *period mapping* of first return to the equator: $p_\theta \mapsto T(p_\theta)$.

The geodesic flow is Liouville integrable and the transcendence is characterized basically by the transcendence of the period mapping. More precisely, to integrate one introduces $X = \sin^2 r$, $r \in (0, \pi/2)$ and one gets

$$\int \frac{dr}{(1 - V(r, p_\theta))^{1/2}} = \int \frac{dx}{2((X(1 - X)(1 - V(X))^{1/2}}.$$

To integrate one can assume that $r(0) = 0, \theta(0) = 0$ since every oscillating trajectory is such that r is intersecting the equator and we use

$$\frac{dr}{dt} = \sqrt{1 - V(r, p_\theta)}$$

$$\frac{d\theta}{dt} = \frac{\partial H}{\partial p_\theta} = \frac{V(r, p_\theta)}{p_\theta}.$$

One gets that

$$\theta(t) = (2n - 1)\Delta\theta + \int_{r(t)}^0 \frac{V(r, p_\theta)\, dr}{p_\theta(1 - V(r, p_\theta))^{1/2}},$$

where $n \in \mathbb{N}$ counts the number of intersections with the equator and by symmetry we can asssume that the number of intersections is odd. The function $\Delta\theta$ for $p_\theta \in (0, m(0)$ is the so-called *first return mapping to the equator*. The following is crucial in our optimality analysis. We can restrict to an initial point at the equator $q_0 = (0, 0)$.

Proposition 4.3. *Assume that the first return mapping to the equator is monotone non increasing, then the first conjugate time is given by the equation*

$$\frac{\partial \theta}{\partial p_\theta}(r, p_\theta) = 0,$$

where θ is parameterized by r according to

$$\theta(r, p_\theta) = \Delta\theta(p_\theta) - \int_{r_+}^r \frac{V(r, p_\theta)}{p_\theta(1 - V(r, p_\theta))^{1/2}}$$

the first conjugate conjugate time being between $T/2$ and $T/2 + T/4$.

Integration of solutions

$$\left(\frac{dr}{dt}\right)^2 = \frac{\cos^2 r - p_\theta^2(1 - \lambda \cos^2 r)}{\cos^2 r}.$$

We denote Z_+ and Z_- the roots of

$$1 + p_\theta^2(\lambda - 1) = Z^2(1 + \lambda p_\theta^2),$$

where $Z = \sin r$ and the period reads

$$\frac{T}{4} = \int_0^{Z_+} \frac{dZ}{(1 + p_\theta^2(\lambda - 1) - Z^2(1 + \lambda p_\theta^2))^{1/2}}.$$

Normalizing the amplitude of the oscillation by $Z = Z_+ Y$ one has

$$\frac{T}{4} = \int_0^1 \frac{dY}{((1 + \lambda p_\theta^2)(1 - Y^2))^{1/2}}$$
$$= \frac{1}{(1 + \lambda p_\theta^2)^{1/2}} [\arcsin Y]_0^1.$$

Proposition 4.4. *The period is given by*

$$T(p_\theta) = \frac{2\pi}{(1 + \lambda p_\theta^2)^{1/2}},$$

moreover one has:

$$\arcsin Y(t) = (1 + \lambda p_\theta^2)^{1/2} t.$$

This defines the renormalized time $s = (1 + \lambda p_\theta)^{1/2} t$ and the θ−variable is integrated using

$$\frac{d\theta}{dt} = p_\theta \frac{1 - \lambda(1 - \sin^2 r)}{1 - \lambda \sin^2 r}.$$

Hence one gets

$$\theta(t) = \int \frac{p_\theta \, dt}{\cos^2 r} - \lambda p_\theta t$$

and we obtained the following.

Proposition 4.5.

$$\theta(t) = \frac{p_\theta}{(1 + \lambda p_\theta^2)^{1/2}(1 - Z_+^2)^{1/2}} atan((1 - Z_+^2)^{1/2} tan(t(1 + \lambda p_\theta^2))) - \lambda p_\theta t.$$

This leads to a complete parameterization of the geodesics curves and of the conjugate locus. Note that a simplify and standard computation is to parameterize the angle θ by r instead of t. Moreover one can compute the periodic curves. Indeed, one can obtain the first return mapping $\Delta\theta(p_\theta)$ by setting in the above formula $t = T/2$ and periodic mappings are such that $\Delta\theta/2\pi$ is a rational number. In particular simple periodic geodesics can be obtained and classified by ordering with respect to their length, by analogy with the prolate ellipsoid case, the shortest being the meridian. In particular, in the averaged Kepler case they are described in [9], that is five *simple* curves. To analyse the optimality in this Riemannian case we procced as follows.

Determination of the conjugate and cut loci We recall that, the problem is called *tame* if the first return mapping to the equator is monotone non increasing.

Proposition 4.6. *In the tame case case the cut locut of a point on the equator is a subarc of the equator and the injectivity radius is formed by the cusp extremity of the conjugate locus on the equator.*

More generally the conjugate and cut loci of each point can be easily determined using an additional computable condition that we describe next. One has the following.

Proposition 4.7. *Assume that we are in the tame case. Moreover suppose that the first return mapping $\Delta\theta$ is such that $\Delta\theta' < 0 < \Delta\theta$" on $]0, m(\pi/2)[$ then:*

1. *The cut locus of a point not a pole is a segment of the antipodal parallel;*

2. *The conjugate locus has exactly four cusps points.*

This can be applied to the our case for $\lambda \in]0, 1[$. Note that the conjugate locus of the equator is a standard astroid with four cusps. The limit Grushin case can be analyzed similarly, except that the equator is not a geodesic and the injectivity radius is zero. This gives a complete analysis of the Riemannian case.

4.2.2 Transition from the Riemannian case to the Zermelo case with a constant current

Recall that the so-called constant current case is given on the covering space by

$$F_0 = v \frac{\partial}{\partial \theta}, \quad g = \mathrm{d}r^2 + m^2(r)\,\mathrm{d}\theta^2,$$

where v is a non zero constant. We are in the:

- Weak case if $\sin^2 r_0 < \frac{1}{v^2 + \lambda}$, with $q_0 = (r_0, \theta_0)$;

- Strong case if $\sin^2 r_0 > \frac{1}{v^2 + \lambda}$, with $q_0 = (r_0, \theta_0)$;

- moderate case if $\sin^2 r_0 = \frac{1}{v^2 + \lambda}$, with $q_0 = (r_0, \theta_0)$;

Assumptions 4.1. *In the case where the constant v is such that $v^2 + \lambda < 1$, the current will be weak at any point of M. Thus in order to be in the strong case, we shall make the additional assumption*

(A1) : $v^2 + \lambda > 1$.

The following is a crucial geometric property.

Proposition 4.8. *On the two-sphere of revolution the vector field F_0 defines a linear vector field on $\mathbb{R}^3$ tangent to the sphere and it corresponds to an uniform rotation whose axis is the axis of revolution. For the metric the equator solution is also a stationary rotation since $\frac{\mathrm{d}\theta}{\mathrm{d}t}$ is constant along of the equator so that the effect of the constant current can be superposed with this rotation.*

To make the analysis we proceed as previously, the parameterization of the geodesics being similar but the effect of the current is to obtain a more complicated mico-local analysis that we describe next, related to vanishing or not of the derivative of $\theta-$component. Here, the Hamiltonian vector field is given by:

$$\mathbf{M} = p_\theta v + \|p\|_g = -\varepsilon, \quad \|p\|_g = \sqrt{p_r^2 + \frac{p_\theta^2}{m^2(r)}}. \tag{24}$$

with $\varepsilon < 0$ (resp. $\varepsilon > 0$) correspond to hyperbolic (resp. elliptic) case and $\varepsilon = 0$ to the abnormal one. we fix by homogeneity $\|p\|_g = 1$, since from the Hamiltonian one has $\|p\|_g = -(\varepsilon + p_\theta v)$ is constant. Moreover $G = p_\theta$ is the additional (linear) first integral and this insured the Liouville integrability of the system. One then gets the following:

Proposition 4.9. *The $r-$dynamics can be integrated using the characteristic equation*

$$\left(\frac{\mathrm{d}r}{\mathrm{d}t}\right)^2 + V_\epsilon(r, p_\theta) = 1$$

where $\varepsilon = -p^0 < 0, = 0, > 0$ correspond respectively to the hyperbolic, abnormal and elliptic case.

Proof. In the constant current case, starting from the equator and using the ascending branch gives the equation

$$\frac{\mathrm{d}r}{\mathrm{d}t} = \left(\frac{p_\theta^2(1 - \lambda \sin^2 r)}{\sin^2 r (\epsilon + p_\theta v)^2}\right)^{1/2},$$

and since we have posed $\|p\|_g = 1$, that is $(\varepsilon + p_\theta v) = -1$, then one has

$$\frac{\mathrm{d}r}{\mathrm{d}t} = \left(\frac{p_\theta^2(1 - \lambda \sin^2 r)}{\sin^2 r}\right)^{1/2},$$

which is the same expression as in the Riemannian case, computation is then similar. □

To integrate θ we use the dynamics

$$\frac{\mathrm{d}\theta(t)}{\mathrm{d}t} = \frac{\partial H}{\partial p_\theta}.$$

Again note that θ can be computed easily, parameterizing by r instead of t and one gets the following proposition. (In particular to determine the first return mapping to the equator).

Proposition 4.10. *The θ-variable is given by:*

$$\theta(t) = (2n-1)\Delta\theta + \int_{r(t)}^{0} \frac{V_\epsilon(r, p_\theta)\, \mathrm{d}r}{p_\theta(1 - V_\epsilon(r, p_\theta))^{1/2}},$$

where $n \in \mathbb{N}$ counts the number of intersections with the equator and by symmetry we can asssume that the number of intersections is odd. The function $\Delta\theta$ for $p_\theta \in (0, m(r_0))$ is the first return mapping to the equator.

This leads to the following stratification of the set of geodesics, using a stratification by the variable p_θ instead of the heading angle in the historical case. Indeed in this case the geodesics curves are reflectionally symmetry with respect to the equator solution, the cone of direction being symmetric with respect to the equator. One can consider only by symmetry the case of ascending branches at the initial condition.

Stratification of the set of geodesics   Suppose that assumption (A1) hold. Starting from the equator and assuming $p_r(0) > 0$, one has the following stratification of the set of geodesics.

Proposition 4.11. *geodesics of $\mathbf{M}$ split into:*

- *Abnormal geodesics : We have two distinct abnormal geodesics parameterized by $p_\theta^a = -1/v$ and $p_{r_0} > 0$ for the ascending one and $p_{r_0} < 0$ for the descending one.*

- *Hyperbolic geodesics : which correspond to the time minimal solutions and parameterized by $p_\theta \in \,]p_\theta^a, m(r_0)[$.*

- *Elliptic geodesics : which correspond to the time maximal solutions and parameterized by $p_\theta \in [-m(r_0), p_\theta^a[$.*

Moreover, in the hyperbolic case, the set of geodesics can be stratified in four classes namely (see Fig. 8):

- *The equator which corresponds to the singular point: $r = \pi/2$, $p_r = 0$ while $p_\theta = m(r)$*

- *The two pseudo-meridians (ascending and descending one) which correspond to the non compact case $\dot{r} > 0$. They are given by $p_\theta = 0$ and $p_r = \pm 1$.*

- *Generic periodic orbits whcih split in two different families namely orbits without loop parametrized by $p_\theta \in \,]0, m(r_0)[$ and orbits with loops, parametrized by $p_\theta \in \,]p_\theta^a, 0[$ and contening by symmetry the orbits associated to $\pm p_r(0)$.*

Determination of the two branches of the conjugate and cut loci   Next we can determine the conjugate locus for a point at the equator. One needs only to aggregate the two branches associated first to cut points and conjugate point related to the abnormal direction as in the historical examples and associated to self-intersections and cusp singularity. Second branch of cut locus is associated to the tame behavior of the first return mapping to the equator and conjugate points computed for simple geodesics using Jacobi equations (observe that the generalized curvature can be easily computed along the equator since r is constant). Finally observe that such points exists for non self-intersecting geodesics but appear after the self-intersection. This leads to the following theorem

Theorem 4.1. *Let suppose that assumption (A1) hold i.e we are in the strong current case along the equator. Then, the cut locus have two distinguished branches, the first branch being form by the abnormals up to their first cusp point and the second branch being a segment of the equator (see Fig.9).*

Deformation of the conjugate locus by homotopy on the constant current v.   Classical algorithm, presented in section 2 is used here to compute the conjugate locus. In order to see the deformation of the conjugate locus by introduction of a constant current, we start by setting $v = 0$ (that correspond to the average Kepler case study in [9]), then increasing the value of v until $\sqrt{1-\lambda}$ (to remains in the weak case), one can clearly observe the deformation (see Fig.10).
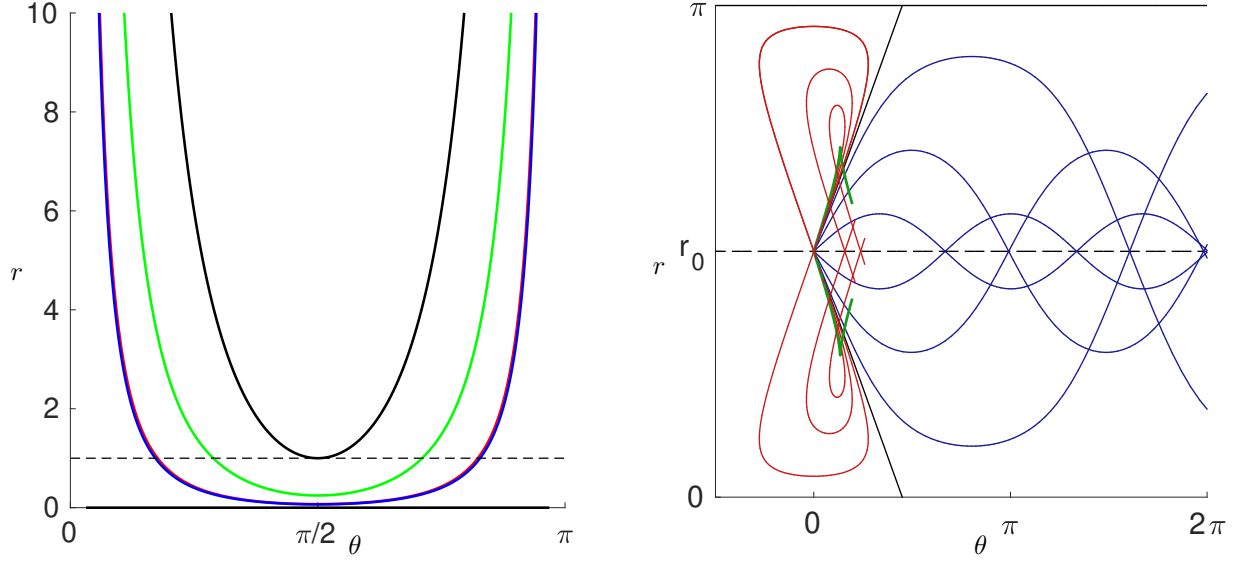
Figure 8: (Left) We represent the potential for the different classes of geodesics in order to highlight the periodicity of the solutions. The meridians and the equator are represented in black while hyperbolic geodesics with a loop (resp. without loop) are represented in red (resp. in blue). Abnormal geodesics are represented in green. (Right) illustration of different types of hyperbolic geodesics in the strong drift case. We take for simulation $\lambda = 4/5$ and $v = 0.9$.
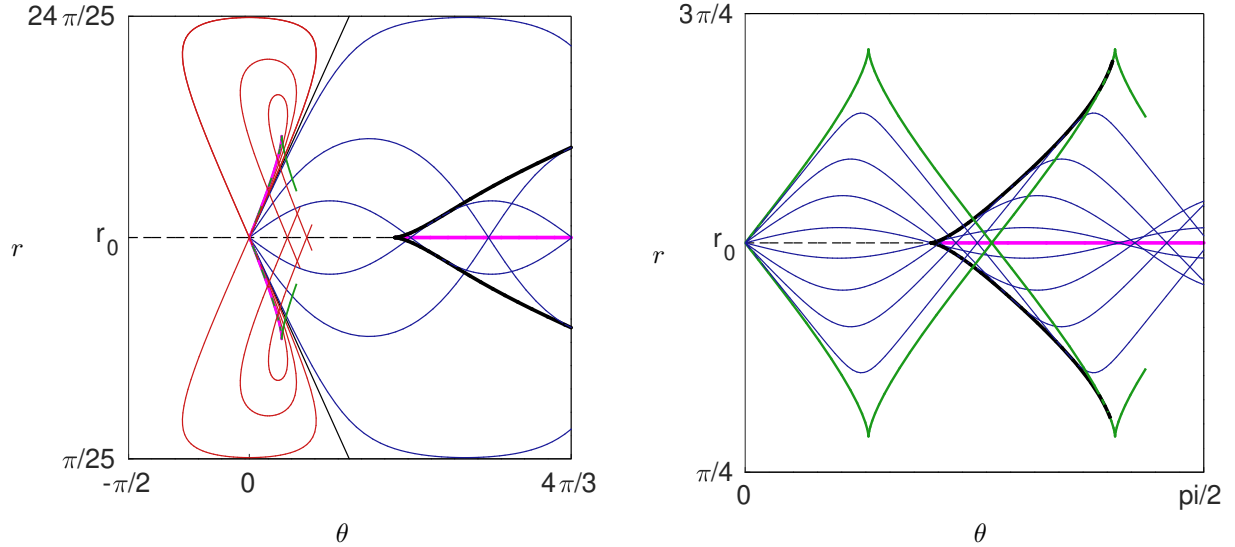

Figure 9: (Right) Minimal time optimal synthese of the average Kepler case with a constant current taking $\lambda = 4/5$ and $v = 0.9$ in adapted rectangle $R = \{\pi/25 \leq r \leq 24\pi/25; -\pi/2 \leq \theta \leq 4\pi/3\}$. The meridians and the equator are represented in black while the hyperbolic geodesics with a loop (resp. without loop) are represented in red (resp. in blue). Abnormal geodesics are represented in green. Conjugate and cut loci are resp. represented in thick black and orange. (Left) Maximal time optimal synthesis in adapted rectangle $R = \{\pi/4 \leq r \leq 3\pi/4; 0 \leq \theta \leq \pi/2\}$. Elliptic geodesics are represented in blue and abnormal ones in green. Conjugate and cut loci are resp. represented in thick black and orange.

4.3 Complexity of the Hamiltonian Dynamics in the generalized vortex case

In the *vortex problem* (see [15] for a complete description of the problem), one has $F_0 = \frac{k}{r^2} \frac{\partial}{\partial \theta}$, with k being circulation parameter, so the current becomes infinite at the vortex (in particular $\alpha_1 = \alpha_2$) but still the
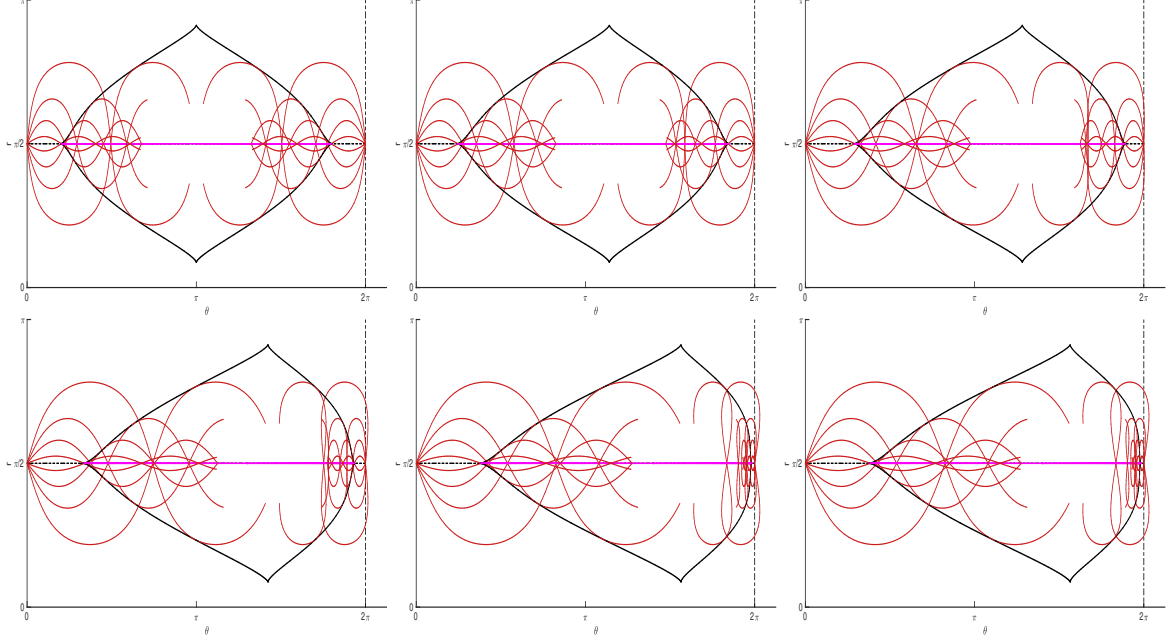
Figure 10: Illustration of the deformation of conjugate locus in weak current case. Taking $\lambda = 4/5$ and $v = 0.0, 0.1, 0.2, 0.3, 0.4, 0.42$ respectively from the left to the right. One can see in red hyperbolic geodesics, in black conjugate locus and in maginta separatine line (that correspond here to cut locus).

dynamics can be extended on the whole plane. We will first consider this case. Then, in order to presented a more completed situation with many equators, compact and non compact geodesics, we will consider the so-called general single-vortex case. But first of all, we start by providing a generalization of the existence theorem from [15], see also the relation with [23] in celestial mechanics.

4.3.1 Existence of optimal solution

In this section we analyze the general vortex case. It takes the form

$$F_0 = \mu(r)\frac{\partial}{\partial\theta}, \qquad F_1 = \frac{\partial}{\partial\theta}, \qquad F_2 = \frac{1}{m(r)}\frac{\partial}{\partial r},$$

In the simple vortex case one has $\mu(r) = \frac{1}{r^2}$. In the general we assume that $\mu(r)$ has a pole of order $\beta \in]1, +\infty]$ at zero so one can take the approximation $\mu(r) \sim \frac{1}{r^\beta}$ near the pole and moreover we assume $\mu(r) \to 0$ when $r \to +\infty$. First of all we need to generalize the argument of [36] to prove the existence of a solution. The proof is related to [36], [23] about the existence of minimizing solutions avoiding collision in the N-body problem and the Levi-Civita regularization of double collisions in the 3-body problem [38], see also [16] as a general reference in the context of existence of optimal solutions in control and Hamiltonian Dynamics. We have the following.

Theorem 4.2. *Take q_0, q_1 in the punctured plane $\mathbb{R}^2 \setminus \{0\}$, then there exists a time minimizing trajectory to transfer q_0 to q_1. Moreover $q_0 = (r_0, \theta_0)$ can be transferred to the origin in minimum time $t_{min} = r_0$. Hence one can extend the geodesic flow using a Levi-Civita type regularization beyong the collision with the pole by reversing the geodesic time parameterization when crossing the vortex.*

ketch of the proof. The geodesic dynamics in polar coordinates reads

$$\frac{dr}{dt} = \frac{p_r}{\|p\|_g},$$
$$\frac{d\theta}{dt} = \mu(r) + \frac{p_\theta}{m^2(r)\|p\|_g}.$$

23

To prove the existence about minimizers curves it is sufficient to prove that the minimizing trajectories are avoiding the collision. Using the expansion near the pole and comparing the time to make a rotation around the pole on a circle of radius r denoted $T_\theta(r)$ and the time to reach a circle of radius r denoted $T_r(r)$ a direct computation gives

$$T_\theta(r) = \frac{2\pi r^\beta m(r)}{r + m(r)}, \quad T_r(r) = r^\beta - \varepsilon.$$

Hence the argument of [1] to replace a trajectory reaching a circle with small radius ε by trajectory making a rotation around the pole is still valid and the existence results follows. Clearly from the equations the time to reach the pole form q_0 is obtained for $p_\theta = 0$ and is given by r_0. Following the Levi-Civita regularization we reverse the geodesics orientations when crossing the vortex. It amounts to replace $\mu(r)$ by $-\mu(r)$ and p_θ by $-p_\theta$ in the geodesics equations. $\square$
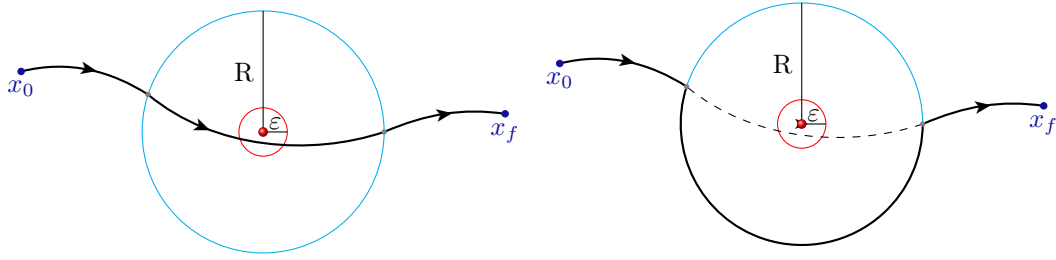

Figure 11: Illustration de la construction d'une trajectoire admissible strictement meilleure. Le vortex est représenté par une boule rouge, tandis que les trajectoires sont les lignes noires pleines. On peut voir à gauche, une trajectoire traversant la boule de rayon ε. Cette trajectoire est remplacée sur le sous-graphe de droite par une trajectoire admissible strictement meilleure.

Remark 2. *In the vortex case the cone of admissible directions tends to zero at the vortex and the system is in the strong current domain. In this case we can encounter geodesics rotating around the vortex to reach a final point and make use of the vortex to reach points [5].*

Remark 3. *One must have $\beta > 1$, so it is similar to the assumption of Poincaré to avoid collisions for minimizers by modifying the Keplerian potential and the bound $\beta \geq 2$ in the potential interaction (called potentiel fort by Poincaré). IOn our case the bound is given by $T_\theta(r) < T_r(r)$ gives $\varepsilon < r\left(1 - \frac{2\pi r^{\beta-1} m(r)}{r^\beta + m(r)}\right)$ for a couple $0 < \varepsilon < r$ and the bracket term has to be > 0.*

Next we describe the complexity of the dynamics in the vortex problem, particular in relations with interaction between equators and the vortex.

4.3.2 The single vortex case in hydrodynamics

On the punctured plane we consider the case of an Euclidiann metric in polar coordinates with $g = dr^2 + r^2 d\theta^2$ and the current given $F_0 = \frac{k}{r^2}\frac{\partial}{\partial\theta}$. The generalized potential is given by

$$V_\varepsilon(r, p_\theta) = \frac{p_\theta^2 r^2}{(\varepsilon r^2 + p_\theta k)^2}.$$

The geodesics curves can be classified using the potential and the main features are described next see [6] for the details.

Theorem 4.3. • *The domain of strong current is near the vortex and limited by the circle with radius $r = k$ of moderate current. The only equator solution is in the domain of weak current and is defined by the circle with radius $r^* = 2k$. There exist an unique sepratrix forming a in the interior of the disk delimited by the equator emanating from the vortex as a singular point and forming a Reeb component of a foliation with singularity emanating from the vortex and converging to the equator where $\frac{d\theta}{dt} = 0$ on the circle with radius $2k/\sqrt{3}$.*

24

- *At the exterior of the circle with radius r^* there exists an unique separatrix emanating from the equator and converging to the infinity.*

- *There exist two pseudo-meridians where $p_\theta = 0$, converging with maximal radial speed either towards the vortex or to the infinity.*
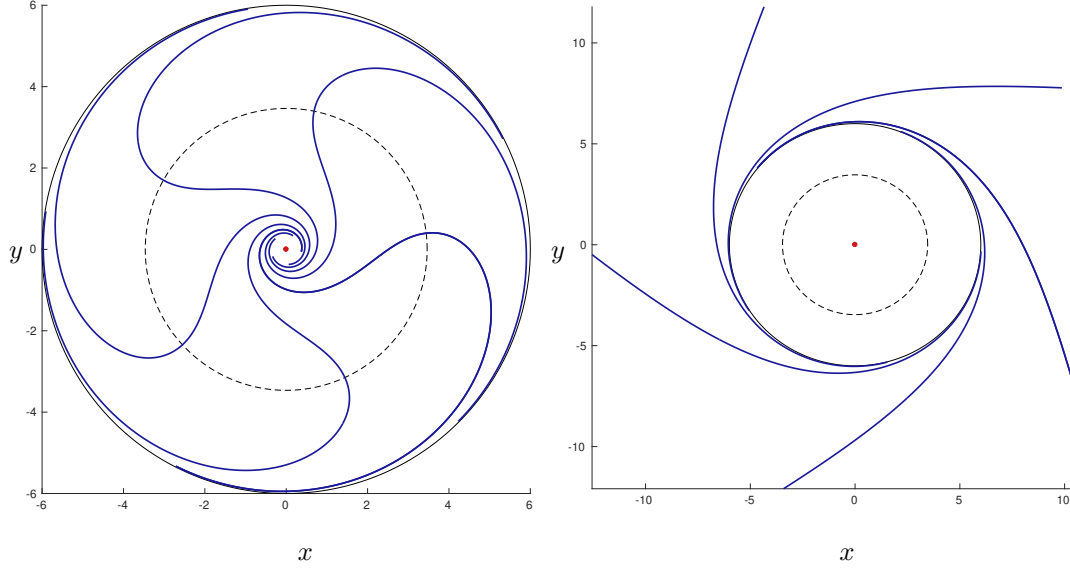

Figure 12: (Gauche) Feuilletage de Reeb formée par les séparatrices dans le disque perforé de rayon $2k$ dans le plan (x, y). (Droite) Feuilletage de Reeb formée par les séparatrices à l'extérieur du disque de rayon $2k$ dans le plan (x, y). Le vortex est placé à l'origine et représenté par un point rouge. Les cercles en noir repré de rayon $2k$ tandis que le cercle noir correspondent resp. aux cercles de rayon $2k/\sqrt{3}$ o(ù $\dot{\theta}$ s'annule le long de la séparatrice) et $2k$.

If we parameterize geodesics by the heading angle, that is fixing $\|p(0)\|_r = 1$ and pose $p_r(0) = \cos\alpha, p_\theta = r_0 \sin\alpha$. Denoted α^* the heading angle assoiciated to the equator, then geodesics can be classified in four different families according to their α and ω-limit sets.

Theorem 4.4 (Classification of geodesic orbits in the simple vortex problem)**.** *For a given $q_0 = (r_0, \theta_0)$, one has:*

- *for $\alpha \in]\alpha^*, 0[$, $(\tilde{\Lambda}^-(q_0), \tilde{\Lambda}^+(q_0)) = (\{0\}, \varnothing)$*

- *for $\alpha \in]0, \pi[$, $(\tilde{\Lambda}^-(q_0), \tilde{\Lambda}^+(q_0)) = (\varnothing, \varnothing)$.*

- *for $\alpha \in]\pi, \pi - \alpha^*[$, $(\tilde{\Lambda}^-(q_0), \tilde{\Lambda}^+(q_0)) = (\varnothing, \{0\})$*

- *for $\alpha \in]\pi - \alpha^*, \alpha^*[$, $(\tilde{\Lambda}^-(q_0), \tilde{\Lambda}^+(q_0)) = (\{0\}, \{0\})$,*

Where we denoted $\tilde{\Lambda}^\pm(z_0)$ the projection on q-space of $\Lambda^\pm(z_0)$.

4.3.3 Single general vortex case

In the simple vortex problem presented above, there is an unique equator for $r_0 = 2\mu$. In order to present a more general and complicated situation where we encounter several separatrices and equators, we consider drift F_0 in the form:

$$F_0(q) = \mu(r)\frac{\partial}{\partial\theta}, \quad \text{with} \quad \mu(r) = \frac{\lambda r + \beta}{r^3}, \quad \lambda, \beta \in \mathbb{R}^*.$$

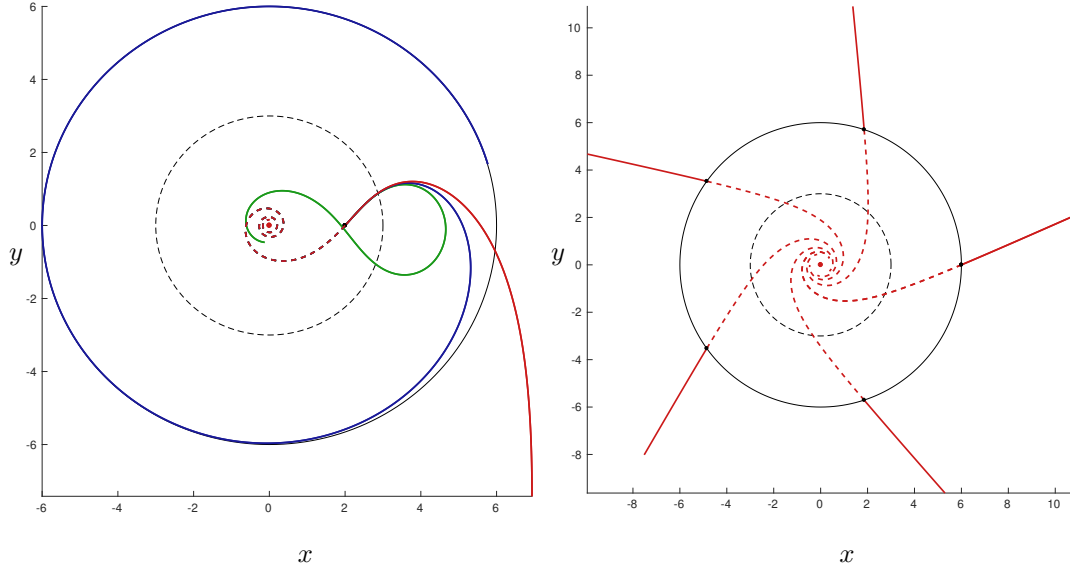According to Proposition. 3.6, equators and separatrices are given by:

Figure 13: (Gauche) Illustration du comportement des géodésiques au voisinage de la séparatrice dans le plan (x, y). Pour les géodésiques en dessous de la séparatrice (représenté en vert), $\dot{r}$ et $\dot{\theta}$ s'annulent le long d'elles et celles-ci convergent vers la singularité (le vortex) tandis que pour les géodésiques au dessus de la séparatrice (représenté en rouge), $\dot{r}$ et $\dot{\theta}$ ne s'annulent pas et celles-ci vont à l'infini en temps infini. La séparatrice est représenté en bleu et les cercles en noir correspondent resp. aux cercles de rayon μ et 2μ. (Droite) illustration d'une trajectoire formant un diaphragme dans le plan (x, y). On intègre la trajectoire à partir du cercle équateur et pour différente valeur de θ_0 (ici $\theta_0 \in \{2k\pi/5;\ k = 0, \cdots, 4\}$. En trait plein les trajectoire sont parcourues en sens positif et en pointillé, elles sont parcourues en sens négatif. Le vortex est représenté par le point rouge et les points initiaux en noir.

Proposition 4.12. *Supposing that $\lambda^2 > 3\beta$ and $\beta < 0$, then we have three different equators given by*

$$r^1 = -\lambda + \sqrt{\lambda^2 - 3\beta}, \quad r^2 = \lambda - \sqrt{\lambda^2 + 3\beta} \quad et \quad r^3 = \lambda + \sqrt{\lambda^2 + 3\beta},$$

such that the equators r^1 and r^3 are L-hyperbolics and the equator r^2 is L-elliptic.

Moreover, to the equators r^1, r^2 and r^3 are respectively associated the geodesics parametrized by :

$$p_\theta^1 = \frac{m(r^1)}{1 + \mu(r^1)m(r^1)}, \quad p_\theta^2 = -\frac{m(r^2)}{1 - \mu(r^2)m(r^2)}, \quad et \quad p_\theta^3 = -\frac{m(r^3)}{1 - \mu(r^3)m(r^3)}.$$

Remark 4. *The geodesics parametrized by p_θ^1 and p_θ^3 are separatrices since they are associated to L-hyperbolic equators, while the one parametrized by p_θ^2 is not and does not even exist for an initial r_0 taken in the neighborhood of r^2 and different of r^2.*

Proof. Recall that, couples (r, p_θ) forming by r-equators and parameterized p_θ of separatrices are solutions of the system:

$$V_\varepsilon(r, p_\theta) = 1 \quad \text{and} \quad \frac{\partial V_\varepsilon}{\partial r}(r, p_\theta) = 0, \quad \text{with} \quad p_\theta \neq 0, \tag{25}$$

and second equation of (25) gives us the second order equation:

$$\delta r^2 + 2\lambda r + 3\beta = 0, \quad \text{with} \quad \delta = sign(p_\theta), \tag{26}$$

Supposing that $\beta < 0, \lambda^2 > 3\beta$, one then has:

- for $\delta = 1$ i.e $p_\theta > 0$, (26) has one unique positive solution given by $r^1 = -\lambda + \sqrt{\lambda^2 - 3\beta}$,

- for $\delta = -1$ i.e $p_\theta < 0$, (26) has two positive solutions given by $r^2 = \lambda - \sqrt{\lambda^2 + 3\beta}$ and $r^3 = \lambda + \sqrt{\lambda^2 + 3\beta}$

26

Using know first equation of (25) one gets:

$$p_\theta^1 = \frac{m(r^1)}{1 + \mu(r^1)m(r^1)}, \quad p_\theta^2 = -\frac{m(r^2)}{1 - \mu(r^2)m(r^2)}, \quad p_\theta^3 = -\frac{m(r^3)}{1 - \mu(r^3)m(r^3)}.$$

$\square$

To stratified the set of geodesics, it is sufficient to observe de behaviors of the potential associated to separatrices (see Fig.14-16).

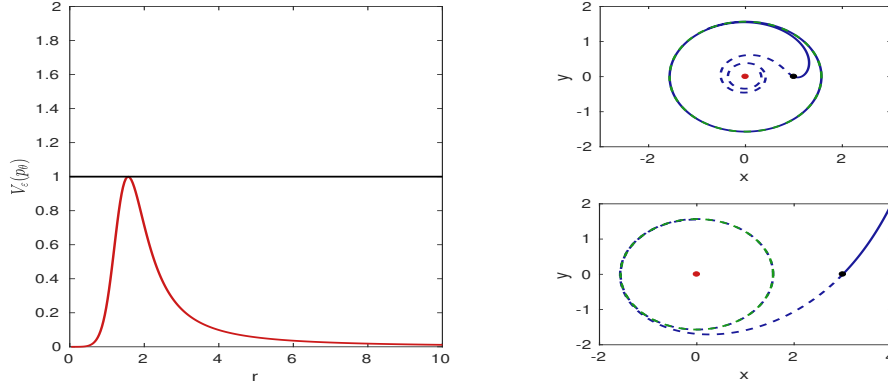Figure 14: Potential along the separatrix (left) and behaviors of separatrix orbit (right). On the right one can see the orbit of separatrix given by p_θ^1 for two different value of r_0. In thick blue orbit is crossed in positive time and in dashed blue it's crossed in negative time. Black dot correspond to the initial position while red dot correspond to the vortex taking as origin.
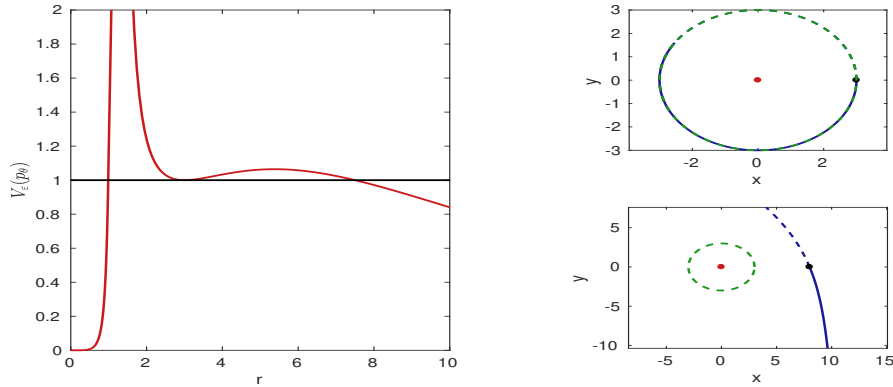

Figure 15: Potential along the separartrix (Left) and behaviors of separatrix orbit (Right). On the right one can see the orbit of separatrix given by p_θ^2 for two different value of r_0. Along p_θ^2 potential explose to infinity for r between 1 and 2. At the right is potrayed the trajectories in the plan for different value of r_0 in order to present the different possibility.

Observations According to Fig.14-16 one can deduce:

- For $p_\theta = p_\theta^1$, potential remains below one. Thus, for $r_0 \leq r^1$ α and ω-limit set of the separatratrix are given by $(\tilde{\Lambda}^-(q_0), \tilde{\Lambda}^+(q_0)) = (\{0\}, \mathcal{C}(0, r^1))$ and for $r_0 > r^1$ one has $(\tilde{\Lambda}^-(q_0), \tilde{\Lambda}^+(q_0)) = (\mathcal{C}(0, r^1), \varnothing)$
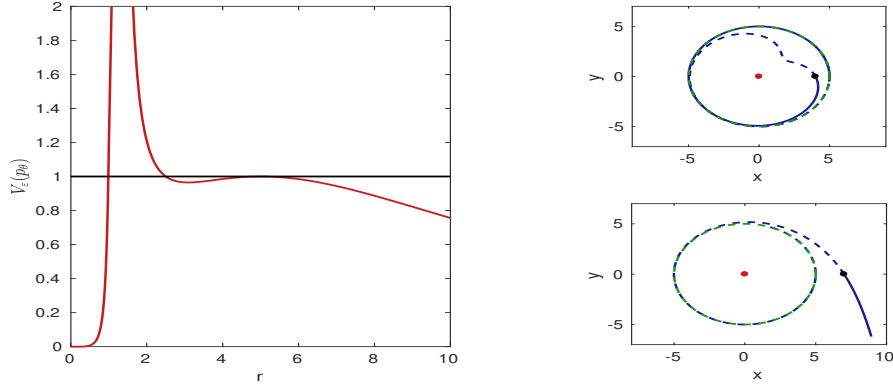
Figure 16: Potential along the separartrix (Left) and behaviors of separatrix orbit (Right). On the right one can see the orbit of separatrix given by p_θ^3 for two different value of r_0. Along p_θ^3 potential explose to infinity for r between 1 and 2. At the right is potrayed the trajectories in the plan for different value of r_0 in order to present the different possibility.

- For $p_\theta = p_\theta^2$, in the neighborhood of r^2, the potential is above one and takes the value one for $r = r^2$. Thus in this neighborhood, separatrix exists if and only if $r_0 = r^2$ and it defines the circle $\mathcal{C}(0, r^2)$.

- For $p_\theta = p_\theta^3$, separatrix exists and is well define for $r_0 \geq 2.5$ and for $r_0 \in [2.5, r^3]$, one has $\tilde{\Lambda}^-(q_0) = \tilde{\Lambda}^+(q_0) = \mathcal{C}(0, r^3)$ while for $r_0 > r^3$, one has $(\tilde{\Lambda}^-(q_0), \tilde{\Lambda}^+(q_0)) = (\mathcal{C}(0, r^3), \varnothing)$

Stratification of geodesics. Representing the potential along the trajectories around the separatrix, we deduce (see Fig.(17)) the different types of orbits encountered in the classification, thus we have:

Proposition 4.13. *Considering the general vortex problem with*

$$F_0(q) = \mu(r)\frac{\partial}{\partial\theta}, \quad with \quad \mu(r) = \frac{\lambda r + \beta}{r^3}, \quad \beta < 0, \quad and \quad \lambda^2 > 3\beta,$$

then orbits of geodesics can be stratified into three types (see Fig.18:

- *Those that come from the vortex (resp. infinity) and go towards the vortex (resp. infinity)*

- *Those that come from the vortex (resp. infinity) and go towards infinity (resp. the vortex),*

- *Those that remain contained in a crown (these correspond to extremals such that $p_\theta \in]p_\theta^2, p_\theta^3[$).*

Different families being delimited by separatrices.

Remark 5. *Thanks to the symmetry which respect to θ we have on one side, separatrix associated to p_θ^1 which form a Reeb foliation (see [7]). On other hand, separatrix associated to p_θ^3 are a typical example of homocline geodesic (i.e for which α and ω-limit set are equal). The behaviors of the both cases are illustrated on Fig.(19).*

4.4 Algorithm in the general case and the gluing process

4.4.1 Algorithm

One can deduce from the previous studies the method of analysis to handle a general case and we proceed as follows. In the normal coordinates (r, θ) on the covering manifold M^c one has $r \in (0, R)$. We can decompose the domains into disks $c_i < r < c_{i+1}$ with alternately weak and strong current. We compute the equators solutions listed as $0 < r_1 < r_2 < ... < r_p < R$ and they can be classified according to their optimality status into hyperbolic or elliptic equators. Taking a point q_0, one can parameterize the geodesics with the mechanical
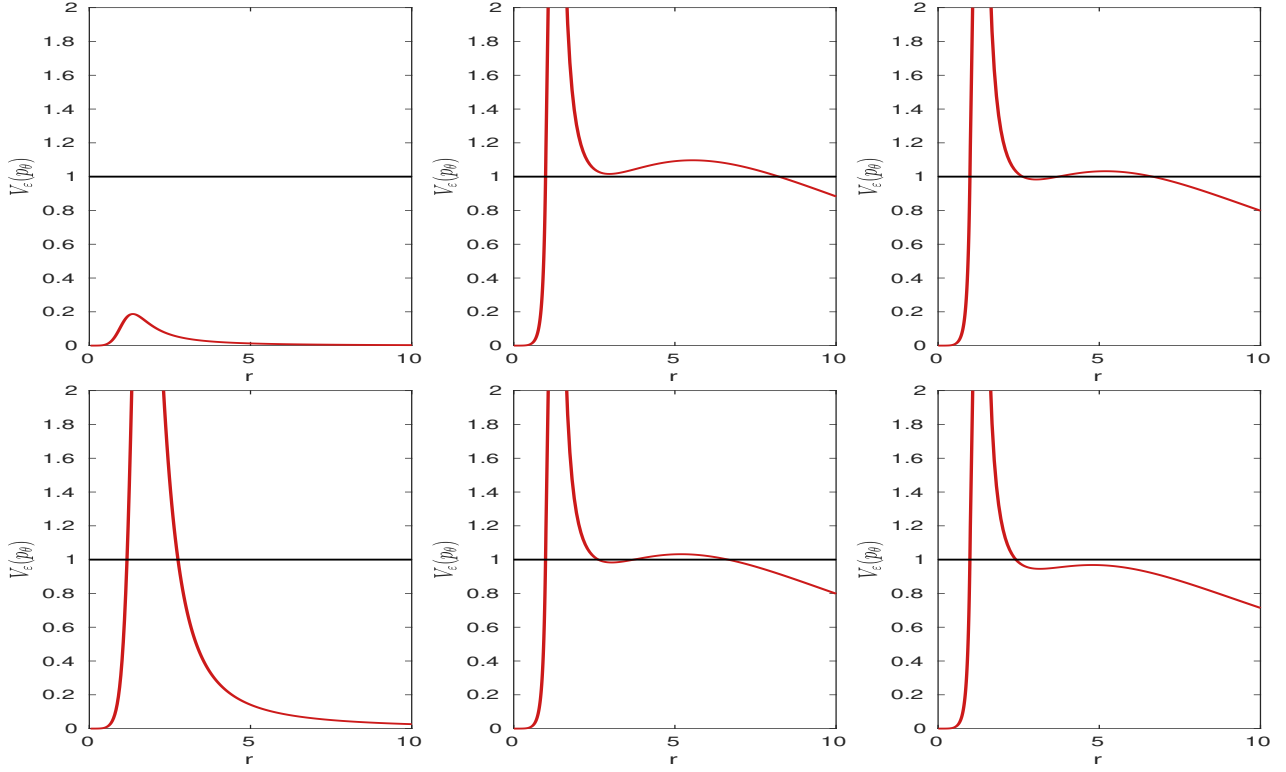
Figure 17: Potential along trajectories around separatrices. Above we consider p_θ less than the p_θ of separatrices, so we take p_θ respectively equal to $p_\theta^1 - 0.5, p_\theta^2 - 0.5$ and $p_\theta^3 - 0.5$. Below we consider p_θ greater than the p_θ of separatrices, so we take p_θ respectively equal to $p_\theta^1 + 0.5, p_\theta^2 + 0.5$ and $p_\theta^3 + 0.5$. For p_θ around p_θ^1 potential remains bounded, but we have, for more clearness of the figure, made a zoom around 1. In other case, potential explose to infinity as in the previous case.
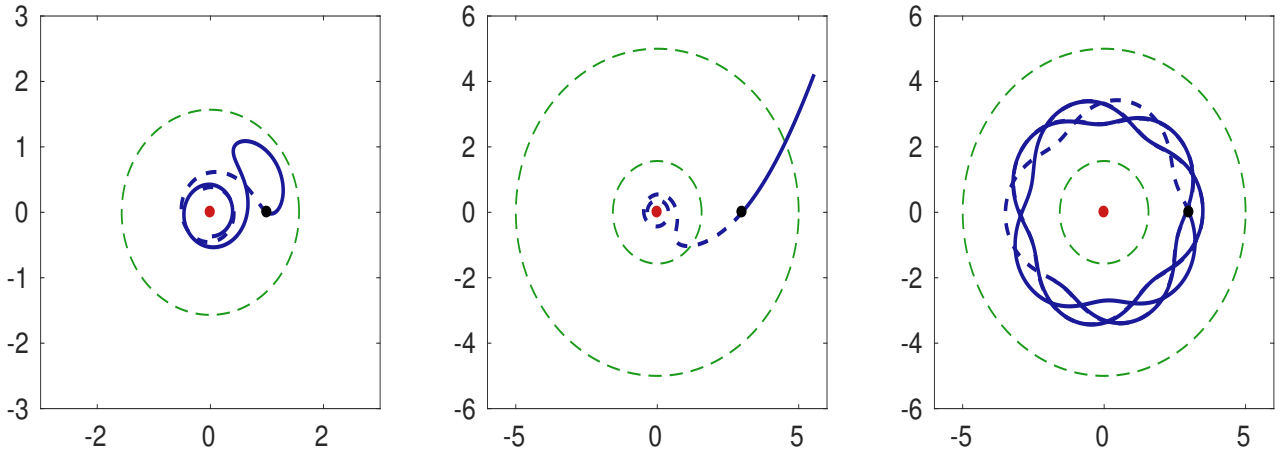

Figure 18: Different families of geodesic orbits, taking $\lambda = 4$ and $\beta = -5$. In thick blue are represented orbits crossed in positive time while in dashed blue orbits are crossed in negative time, start from the given initial point represented by black dot. Red dot represented the vortex. On the left we have an orbit which comes from and go towards the vortex; on the middle we have an orbit which comes from vortex and go towards infinity; and on the right we have a dense orbit which remains in a compact.

representation with the extended potential using *improper integrals*. This allows to construct the time-minimal synthesis in *an adapted neighborhood* as in the cases studies using the first return mappings to the equator and meridian, combining with conjugate point analysis. Note that in the strong current domain the size of the
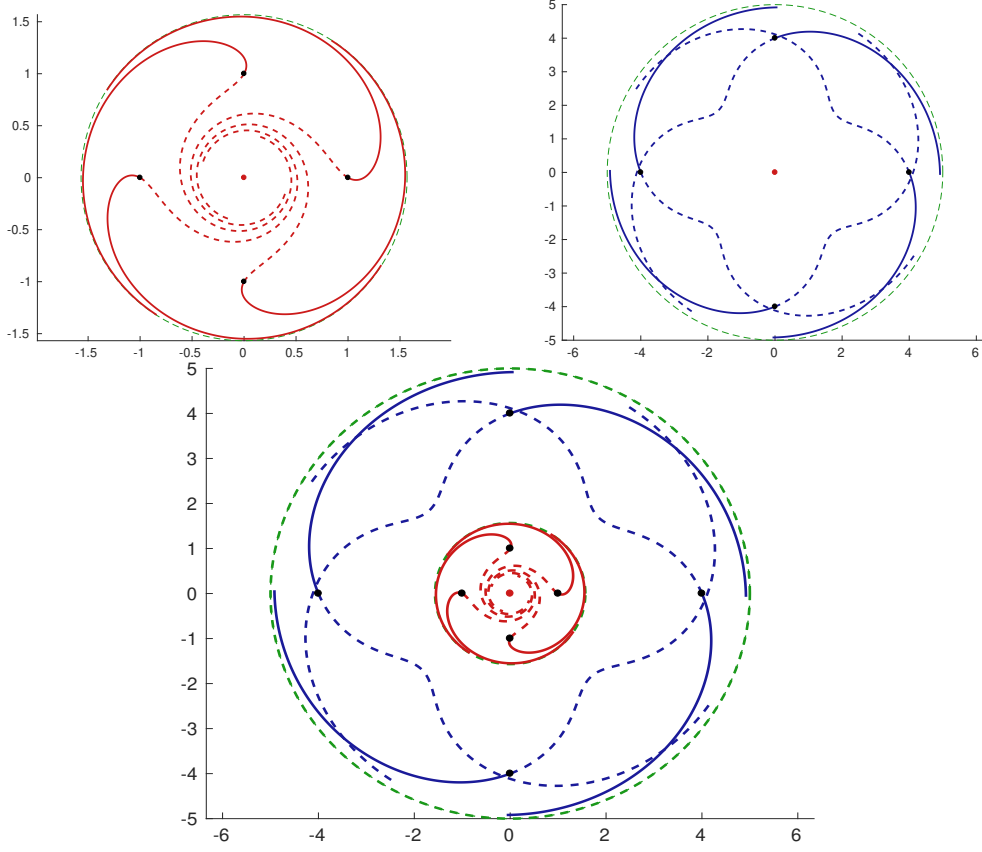
29

Figure 19: Illustration of Reeb foliation forming by separatrix orbits, taking $\lambda = 4$ and $\beta = -5$. Above left we have Reeb component parametrized by p_θ^1 and above right we have homocline separatrix parametrized by p_θ^3. Below the both are potrayed together. In thick correspond the trajectories crossed in positive time and in dashed trajectories crossed in negative time. Red dot correspond to the vortex and black ones to the different initial points we have consider. Circle in green represent the two Reeb circle associated to r^1 and r^3.

adapted neighborhood is defined by the limit loop of the self-intersecting geodesics related to the abnormal direction. This can be extended to a larger domain by gluing different adapted neighborhoods.

4.4.2 The gluing process

Note that complicated situations can be obtained by gluing cases studies using the normal coordinates (r, θ), each case being defined by a pair $(\mu_i(r), m_i(r))$ parameterizing respectively the current and the metric. They can be glued together in the $\mathbb{C}^\infty$-category using bump functions . For instance the vortex case with Euclidian metric can be glued to the averaged Kepler case to represent the motion of a passsive tracer swallowed by the vortex to enter into a Kepler domain to visit an equator solution, with non zero-curvature.

References

[1] A. A. Agrachev & Y. L. Sachkov, *Control theory from the geometric view-point*, vol **87** of *Encyclopaedia of Mathematical Sciences*, Springer-Verlag, Berlin (2004), xiv+412.

[2] A. Agrachev, N.N. Chtcherbakova, I. Zelenko, *On curvatures and focal points of dynamical Lagrangian distributions and their reductions by first integrals,* J. Dyn. Control Syst. **11** (2005), no. 3, pp. 297–327.

[3] V. I. Arnold & B. A. Khesin, *Topological Methods in Hydrodynamics*, vol 125 of Applied Mathematical Sciences, Springer-Verlag New York, 1998, 376 pages.

[4] V.I. Arnol'd, *Mathematical methods of classical mechanics,* Translated from the Russian by K. Vogtmann and A. Weinstein. Second edition. Graduate Texts in Mathematics, **60**. Springer-Verlag, New York, (1989), xvi+508 pp. ISBN: 0-387-96890-3.

[5] D. Bao, S.-S. Chern & Z. Shen, *An Introduction to Riemann-Finsler Geometry,* vol 200 of Graduate Texts in Mathematics, Springer-Verlag New York, 2000, 435 pages.

[6] D. Bao, C. Robles & Z. Shen, *Zermelo navigation on Riemannian manifolds*, J. Differential Geom., **66** (2004), no. 3, pp. 377–435.

[7] A. V. Bolsinov, A. T. Fomenko, *Integrable Hamiltonian Systems, Geometry, Topology, Classification,*, Chapman and Hall/CRC, London, 2004.

[8] B. Bonnard, J.B. Caillau, *Geodesic flow of the averaged controlled Kepler equation,* Forum Math. **21** (2009), no. 5, pp. 797–814.

[9] B. Bonnard, J. B. Caillau, G. Janin, *Conjugate-cut loci and injectivity domains on two-spheres of revolution.*, ESAIM: COCV **19** (2013), no. 2, pp. 533–554.

[10] B. Bonnard, J. B. Caillau, R. Sinclair, M. Tanaka, *Conjugate and cut loci of a two-sphere of revolution with application to optimal control*, Ann. Inst. H. Poincaré Anal. Non Linéaire 26 (2009), no. 4, 1081-1098.

[11] B. Bonnard & M. Chyba, *Singular trajectories and their role in control theory*, vol **40** of *Mathematics & Applications*, Springer-Verlag, Berlin (2003), xvi+357.

[12] B. Bonnard, O. Cots, N. Shcherbakova, *Riemannian metrics on 2D-manifolds related to the Euler-Poinsot rigid body motion,* ESAIM: COCV **20** (2014), no. 3 pp. 864–893. https://doi.org/10.1051/cocv/2013087

[13] C. Balsa, O. Cots, J. Gergaud, B. Wembe, *Minimum energy control of passive tracers advection in point vortices flow.* In: Gonçalves J.A., Braz-César M., Coelho J.P. (eds) CONTROLO 2020. Lecture Notes in Electrical Engineering, vol 695. Springer, Cham. https://doi.org/10.1007/978-3-030-58653-9_22

[14] B. Bonnard, O. Cots, J. Gergaud, B. Wembe, *Abnormal Geodesics in 2D-Zermelo Navigation Problems in the Case of Revolution and the Fan Shape of the Small Time Balls*, HAL Id : hal-02437507 (2020), Submitted at System Control & Letters.

[15] B. Bonnard, O. Cots & B. Wembe, *A Zermelo Navigation Problem with a Vortex Singularity*, ESAIM: COCV, **27** (2021) no 10, pp: 1-37, https://doi.org/10.1051/cocv/2020058

[16] B. Bonnard, L. Faubourg & E. Trélat, *Mécanique céleste et contrôle des véhicules spatiaux*, vol **51** of Mathématiques & Applications, Springer-Verlag Berlin, 2006, 276 pages.

[17] B. Bonnard, I. Kupka, *Théorie des singularités de l'application entrée/sortie et optimalité des trajectoires singulières dans le problème du temps minimal*, Forum Math., **5** (1993), no. 2, pp. 111–159.

[18] B. Bonnard, D. Sugny, *Time-minimal control of dissipative two-level quantum systems: the integrable case,* SIAM J. Control Optim. **48** (2009), no. 3, pp. 1289–1308. (Reviewer: Paolo Mason) 82C10 (49K15 70Q05).

[19] U. Boscain, B. Piccoli, *Optimal syntheses for control systems on 2-D manifolds*, Mathématiques & Applications (Berlin) [Mathematics & Applications], **43**. Springer-Verlag, Berlin, (2004), xiv+261 pp

[20] A. E. Bryson & Y.-C. Ho, *Applied optimal control*, Hemisphere Publishing, New-York, 1975.

[21] J.-B. Caillau, O. Cots & J. Gergaud, *Differential continuation for regular optimal control problems*, Optimization Methods and Software, **27** (2011), no. 2, pp. 177–196.

[22] C. Carathéodory, *Calculus of Variations and Partial Differential Equations of the First Order, Part 1, Part 2,* Holden-Day, San Francisco, California, 1965–1967; Reprint: 2nd AMS printing, AMS Chelsea Publishing, Providence, RI, USA, 2001, 412 pages.

[23] W. B. Gordon *A minimizing property of Keplerian orbits,* AMS, **99** (1977), no 5, pp. 962-971

[24] V. Grines, E. Gurevich, O. Pochinka, D. Malyshev, *On topological classification of Morse-Smale diffeomorphisms on the sphere* $\mathbb{S}^n, (n > 3)$, Nonlinearity **33** (2020), no. 12, pp. 7088–7113.

[25] R. Hama, J. Kasemsuwan & S. V. Sabau, *The cut locus of a Randers rotational 2-sphere of revolution*, Publ. Math. Debrecen, **93** (2018), no 3-4, pp. 387–412.

[26] R. Hama, S. V. Sabau, *The Geometry of a Randers Rotational Surface with an Arbitrary Direction Wind*, Mathematics, **8** (2020), no. 11, pp. 2047, https://doi.org/10.3390/math8112047.

[27] J. Itoh and K. Kiyohara, *The cut loci and the conjugate loci on ellipsoids*, Manuscripta math., **114** (2004), no. 2, pp. 247–264.

[28] L. D. Landau and E. M. Lifshitz, *Mechanics,* Course of Theoretical Physics, **1** (1976), 3rd ed, Pergamon, Oxford, 1976.

[29] R.K. Meyer, G.R. Hall, *Introduction to Hamiltonian dynamical systems and the N-body problem* Applied Mathematical Sciences, Springer-Verlag, New York, **90** (1992), xii+292, pp. 101–120.

[30] S.B. Myers, *Connections between differential geometry and topology. I. Simply connected surfaces,* Duke Math. J. 1, **3** (1935), pp. 376–391. doi:10.1215/S0012-7094-35-00126-0.

[31] S.B. Myers, *Connections between Differential Geometry and Topology,* Proceedings of the National Academy of Sciences of the United States of America, **21** (1935), no. 4, pp. 225–227.

[32] J.Jr. Palis, de Melo, *Welington Geometric theory of dynamical systems, An introduction,* Translated from the Portuguese by A. K. Manning. Springer-Verlag, New York-Berlin, (1982), xii+198 pp. ISBN: 0-387-90668-1

[33] M.M. Peixoto, *Structural stability on two-dimensional manifolds,* Topology **1** (1962), pp. 101–120.

[34] M.M. Peixoto, *On the classification of flows on 2-manifolds,* Dynamical systems (Proc. Sympos., Univ. Bahia, Salvador, 1971), (1973), pp. 389–419. Academic Press, New York.

[35] H. Poincaré, *Sur les lignes géodésiques des surfaces convexes. (French) [On the geodesic lines of convex surfaces]* Trans. Amer. Math. Soc. **6** (1905), no. 3, pp. 237–274.

[36] H. Poincaré, Œuvres complète, Editions Jacques Gabay sceaux, 1965.

[37] L. S. Pontryagin, V. G. Boltyanskiĭ, R. V. Gamkrelidze & E. F. Mishchenko, *The Mathematical Theory of Optimal Processes*, Translated from the Russian by K. N. Trirogoff, edited by L. W. Neustadt, Interscience Publishers John Wiley & Sons, Inc., New York-London, 1962.

[38] C.L. Siegel, J.K. Moser, *Lectures on celestial mechanics*, Translation by Charles I. Kalme. Die Grundlehren der mathematischen Wissenschaften, Band 187. Springer-Verlag, New York-Heidelberg, 1971. xii+290 pp.

[39] K. Shiohama, T. Shioya, M. Tanaka, *The geometry of total curvature on complete open surfaces,* Cambridge Tracts in Mathematics, Cambridge University Press, Cambridge, **159** (2003), pp. x+284 ISBN: 0-521-45054-3 (Reviewer: Victor Bangert)

[40] H.J Sussmann, *Regular synthesis for time-optimal control of single-input real analytic systems in the plane,* SIAM J. Control Optim. **25** (1987), no. 5, pp. 1145–1162. (Reviewer: Ronald Hirschorn) 93B50 (34C40 49B36)

[41] H.J Sussmann, *RThe structure of time-optimal trajectories for single-input systems in the plane: the C1 nonsingular case.* SIAM J. Control Optim. **25** (1987), no. 2, pp. 433–465. (Reviewer: P. Brunovský) 49B36 (49C20 58A35 93C10 93C15)

[42] E. Zermelo, *Über das Navigations problem bei ruhender oder veränderlicher wind-verteilung*, Z. Angew. Math. Mech., **11** (1931), no. 2, pp. 114–124.